

# The *P. falciparum* alternative histones Pf H2A.Z and Pf H2B.Z are dynamically acetylated and antagonized by PfSir2 histone deacetylases at heterochromatin boundaries

Suffian Azizan,<sup>1,2</sup> Shamista A. Selvarajah,<sup>1,2</sup> Jingyi Tang,<sup>3</sup> Myriam D. Jeninga,<sup>4</sup> Danae Schulz,<sup>5</sup> Kapil Pareek,<sup>4</sup> Tamara Herr,<sup>4</sup> Karen P. Day,<sup>2,6</sup> Tania F. De Koning-Ward,<sup>3</sup> Michaela Petter,<sup>4</sup> Michael F. Duffy<sup>2,6</sup>

**AUTHOR AFFILIATIONS** See affiliation list on p. 18.

**ABSTRACT** The *Plasmodium falciparum* alternative histones Pf H2A.Z and Pf H2B.Z are enriched in the same nucleosomes in intergenic euchromatin but depleted from heterochromatin. They occupy most promoters but are only dynamically associated with expression at *var* genes. In other organisms, acetylation of H2A.Z is important for its functions in gene expression and chromatin structure. Here, we show that acetylated Pf H2A.Z and Pf H2B.Z are dynamically associated with gene expression at promoters. In addition, acetylated Pf H2A.Z and Pf H2B.Z are antagonized by the sirtuin class III histone deacetylases (HDAC) PfSir2A and B at heterochromatin boundaries and encroach upon heterochromatin in parasites lacking PfSir2A or B. However, the majority of acetylated Pf H2A.Z and Pf H2B.Z are deacetylated by class I or II HDACs. Acetylated Pf H2A.Z and Pf H2B.Z are also dynamically associated with promoter activity of both canonical upstream *var* gene promoters and *var* gene introns. These findings suggest that both acetylated Pf H2A.Z and Pf H2B.Z play critical roles in gene expression and contribute to maintenance of chromatin structure at the boundaries of subtelomeric, facultative heterochromatin, critical for the variegated expression of genes that enable rapid adaptation to altered host environments.

**IMPORTANCE** The malaria parasite *Plasmodium falciparum* relies on variant expression of members of multi-gene families as a strategy for environmental adaptation to promote parasite survival and pathogenesis. These genes are located in transcriptionally silenced DNA regions. A limited number of these genes escape gene silencing, and switching between them confers variant fitness on parasite progeny. Here, we show that PfSir2 histone deacetylases antagonize DNA-interacting acetylated alternative histones at the boundaries between active and silent DNA. This finding implicates acetylated alternative histones in the mechanism regulating *P. falciparum* variant gene silencing and thus malaria pathogenesis. This work also revealed that acetylation of alternative histones at promoters is dynamically associated with promoter activity across the genome, implicating acetylation of alternative histones in gene regulation genome wide. Understanding mechanisms of gene regulation in *P. falciparum* may aid in the development of new therapeutic strategies for malaria, which killed 619,000 people in 2021.

**KEYWORDS** malaria, variant histones, chromatin, epigenetics, regulation of gene expression

*Plasmodium falciparum* is the pathogen responsible for the most severe forms of malaria and for the vast majority of the approximately 619,000 deaths in 2021 attributed to malaria (1). *P. falciparum* has a complex lifecycle involving two hosts and

**Editor** Dominique Soldati-Favre, University of Geneva, Geneva, Switzerland

Address correspondence to Michael F. Duffy, mduffy@unimelb.edu.au, or Michaela Petter, michaela.petter@uk-erlangen.de.

Suffian Azizan and Shamista A. Selvarajah contributed equally to this article. S. Azizan performed experimental work and analysis, prepared figures, and contributed to the manuscript; S. Selvarajah did the initial characterization of the antibodies and the wild-type parasite ChIPseq. Azizan did more, but the large contribution of Selvarajah warrants equal co-first authorship.

The authors declare no conflict of interest.

See the funding table on p. 18.

**Received** 28 July 2023

**Accepted** 18 September 2023

**Published** 26 October 2023

Copyright © 2023 Azizan et al. This is an open-access article distributed under the terms of the [Creative Commons Attribution 4.0 International license](https://creativecommons.org/licenses/by/4.0/).

multiple morphological forms that inhabit different intra- and extra-cellular environments within these hosts. The parasite switches on transcription of suites of genes to adapt to these altered environments, and in the 48-hour asexual intra-erythrocytic cycle, the parasite expresses the majority of its genes in a transcriptional cascade that has several bursts of abundance at stage transitions (2, 3). The parasite has a relatively low number of known specific transcription factors (4, 5) and thus may rely heavily on chromatin to regulate this cascade of gene expression. The parasite maintains most of its genome in an atypically euchromatic state characterized by the enrichment of acetylated canonical histones, except in restricted heterochromatic domains at the telomeres and at several chromosome-internal sites (6).

A key feature of asexual *P. falciparum* chromatin is the intergenic enrichment in euchromatin of the alternative histones Pf H2A.Z and Pf H2B.Z and their depletion from heterochromatin (7–10). The alternative histone Pf H2A.Z is conserved throughout evolution except for its divergent N-terminal tail, while Pf H2B.Z is unique to apicomplexans. *P. falciparum* promoters are enriched with nucleosomes containing both Pf H2A.Z and Pf H2B.Z (7–10) consistent with a role for Pf H2A.Z/Pf H2B.Z in promoter structure and gene regulation. Pf H2A.Z and Pf H2B.Z levels typically do not fluctuate nor correlate with the timing of gene transcription (7–10), but promoters with the highest levels of Pf H2A.Z are the most highly transcribed at some point during the intra-erythrocytic lifecycle (7, 11). Similarly, in *Saccharomyces cerevisiae*, high levels of H2A.Z at promoters are required for expression of many genes despite an anti-correlation with temporal transcription (12). These findings suggest an evolutionarily conserved role for H2A.Z in defining the potential of regulatory regions to drive gene expression.

H2A.Z plays diverse roles in chromatin structure, heterochromatin maintenance, mitosis, DNA repair, and gene expression. Contradictory effects on gene expression have been reported for H2A.Z, consistent with differing reports on its effects on nucleosome stability (13–15), but in the most recent cryo-EM study, H2A.Z incorporation decreased nucleosome stability (15). Inactive human promoters are enriched in H2A.Z, which is evicted upon gene induction (14). The position of H2A.Z nucleosomes within promoters seems to be critical for their effect upon gene expression. Poorly positioned H2A.Z nucleosomes are associated with gene repression, whereas a strongly positioned +1 H2A.Z-containing nucleosome is associated with high levels of gene expression (16). Acetylation of metazoan H2A.Z reduces nucleosome stability (17), and destabilization is markedly increased when other histones in the nucleosome are also acetylated (18). As chicken, yeast, and human promoters as well as human enhancers are activated, their acetylated H2A.Z levels increase, and their levels of unmodified H2A.Z decrease (19–24). These observations are consistent with a model where unmodified H2A.Z-containing nucleosomes mark promoters that are then activated when the nucleosomes are destabilized by H2A.Z acetylation. How the destabilized H2A.Z is evicted from active promoters remains unclear, but the pre-initiation complex (PIC) itself is required to remove H2A.Z from nucleosomes at promoters (25), and the ATP-dependent chromatin remodeler INO80 can distort DNA to preferentially replace H2A.Z with H2A in yeast (26). The N-terminal tails of Pf H2B.Z and Pf H2A.Z are heavily acetylated (27–31), which suggests that these acetylated *P. falciparum* alternative histones may play a similar, important, and functional role in *P. falciparum* gene regulation.

Recently, a number of novel regulatory complexes were identified through affinity of their bromodomain protein (BDP) components for different *P. falciparum* histone acetylations (32). The combinatorial interactions between these complexes and the specific transcription factors would go some way toward explaining the tightly regulated transcriptional cascade of otherwise euchromatic genes. For example, the specific transcription factor AP2-I and the bromodomain protein PfBDP1 between them coordinate expression of a subset of erythrocyte invasion genes, but both factors also function independently to regulate other genes (33, 34). PfBDP1 interacts with two other bromodomain proteins, PfBDP2 and PfBDP7 (32, 33, 35), and the complex binds strongly

to multi-acetylated peptides derived from the alternative histones Pf H2A.Z and Pf H2B.Z (32).

The restricted islands of *P. falciparum* facultative heterochromatin that are depleted of Pf H2A.Z/Pf H2B.Z nucleosomes in asexual parasites are enriched in multi-gene families including the *var* genes that encode the immunodominant, variant antigen, and cytoadhesin PfEMP1 (8). A single *var* gene is expressed at one time in a process dependent upon silencing of the rest of the *var* repertoire by the PfSir2 sirtuin and PfHda2 histone deacetylases (36–39). Uniquely among *P. falciparum* genes, the *var* gene promoters are dynamically enriched in Pf H2A.Z/Pf H2B.Z nucleosomes in association with *var* gene expression (8). *Var* gene introns also have a regulatory function driving the expression of regulatory ncRNAs (40, 41) and are also enriched in Pf H2A.Z/Pf H2B.Z nucleosomes (8, 10); however, this is unlinked to the activity of the upstream promoter. The removal of Pf H2A.Z/Pf H2B.Z nucleosomes from transiently repressed *var* gene promoters is dependent on the histone deacetylase PfSir2A (8). In *S. cerevisiae*, H2A.Z plays a crucial role for genomic chromatin structure by antagonizing the spread of Sir2-dependent telomeric heterochromatin (42, 43), and it also antagonizes sirtuin-dependent gene silencing (44). It is plausible that Pf H2A.Z/Pf H2B.Z nucleosomes play a similar important role in confining *P. falciparum* facultative heterochromatin.

Here, we show that acetylated Pf H2A.Z (Pf H2A.Zac) and acetylated Pf H2B.Z (Pf H2B.Zac) are dynamically associated with gene expression across the *P. falciparum* genome. This suggests that Pf H2A.Z/Pf H2B.Z nucleosomes help define promoters and that their acetylation could recruit transcription regulating complexes or destabilize the nucleosomes leading to activation of the underlying promoter. We also show that the ablation of PfSir2A results in nucleosomes containing Pf H2A.Zac/Pf H2B.Zac encroaching on heterochromatin boundaries, suggesting that at sites of facultative heterochromatin, sirtuins antagonize the alternative histones and their acetylation. However, ablation of PfSir2A or PfSir2B has no significant effect on the alternative histones beyond the heterochromatin boundaries with the distribution of both acetylated and total Pf H2A.Z and Pf H2B.Z unaffected in euchromatin and still largely excluded from within the facultative heterochromatin domains. Pf H2A.Zac and Pf H2B.Zac are also enriched in introns of *var* genes in association with sterile second exon transcripts. Overall, these patterns suggest that Pf H2A.Zac and Pf H2B.Zac play a critical role in establishing functional chromatin structure in these subtelomeric regions.

## RESULTS

### Generation and characterization of Pf H2A.ZK11K15ac- and Pf H2B.ZK3K8ac-specific antibodies

Pf H2A.Z and Pf H2B.Z are acetylated at multiple sites in their N-terminal tails (27–31). To study the function of variant histone acetylation in *P. falciparum*, we designed peptides that cover non-redundant acetylated epitopes in the N-terminal tails of the two variant histones (Fig. 1A). Some acetylated epitopes occurring in Pf H2A.Z are also present in H4 (LGKacGG and GKacGGKacG motifs), as evident from the cross-reactivity of H4K12ac antibodies with Pf H2A.Z (8) (Fig. 1B). Therefore, the region L21 to G29 was avoided, and a peptide covering Pf H2A.Z amino acids 6–18 and containing two repeats of the Pf H2A.Z-specific GGKacVGG epitope (Pf H2A.ZK11K15ac) was synthesized. Pf H2B.Z shares an AKKT motif with H2B covering K13 and K14, so a peptide covering the Pf H2B.Z-specific N-terminal acetylation sites at K3 and K8 was synthesized (Pf H2B.ZK3K8ac). Both peptides were conjugated to keyhole limpet hemocyanin and used to immunize rabbits (Anaspec) (Fig. 1A). To isolate acetyl-specific anti-Pf H2A.ZK11K15ac and anti-Pf H2B.ZK3K8ac antibodies, the rabbit antisera were incubated with immobilized acetylated peptides, and the bound antibodies were eluted and cross-adsorbed against immobilized, non-acetylated peptides. Pan-reactive antibodies able to recognize both acetylated and unacetylated forms of Pf H2B.Z variants were then obtained from the fraction bound to the non-acetylated peptides (anti-pan-Pf H2B.Z). As the anti-pan-Pf H2A.Z antibody did not detect the unacetylated Pf H2A.Z peptides (not shown), we instead used an

anti-Pf H2A.Z antiserum in this study, which we had previously shown bound both unacetylated and acetylated forms of Pf H2A.Z (8).

The specificity for alternative histones of antibodies to acetylated Pf H2A.Z or Pf H2B.Z or to anti-Pf H2B.Z was confirmed using Western blots of *P. falciparum* histone extract (Fig. 1B). Moreover, the specificities of the purified anti-Pf H2A.Zac and anti-Pf H2B.Zac antibodies for the acetylated forms of Pf H2A.Z and Pf H2B.Z, and of the purified anti-pan-Pf H2B.Z antibodies for both acetylated and unacetylated Pf H2B.Z were confirmed by probing dot blots of unconjugated acetylated and unacetylated peptides of the same sequence as used for immunization (Fig. 1C and D). The anti-Pf H2A.Zac and anti-Pf H2B.Zac antibodies also did not react with a range of single- and multiple-acetylated H3 and H4 peptides by dot blot (Fig. S1).

### The location of acetylated Pf H2A.Z and Pf H2B.Z correlates with the location of total Pf H2A.Z and Pf H2B.Z

*P. falciparum* wild-type 3C parasites that were selected from 3D7 to predominantly express the *var2csa* gene (45) were analyzed by cross-linked chromatin immunoprecipitation followed by DNA sequencing (ChIPseq) to identify genomic sites where Pf H2A.Z and Pf H2B.Z were acetylated. In both ring- and schizont-stage parasites, Pf H2A.Z and Pf H2B.Z were highly correlated. Pf H2A.Zac and Pf H2B.Zac were highly correlated in schizonts and moderately correlated in ring stages due to variation between the Pf H2B.Zac ring-stage replicates (Fig. S2A). These observations were consistent with the published exclusive co-occupancy of nucleosomes by Pf H2A.Z and Pf H2B.Z and further suggested that if one variant was acetylated, the other likely was as well. In both ring and schizont parasites, the total levels of each alternative histone also correlated well with the levels of its acetylated forms (all Spearman  $r > 0.62$ ) (Fig. S2A and B), suggesting that at most sites where Pf H2A.Z and Pf H2B.Z were present, some of the Pf H2A.Z and Pf H2B.Z were acetylated.

### Acetylated Pf H2A.Z and Pf H2B.Z are enriched in intergenic euchromatin

We used H3K9me3 broad peaks called from 3D7 ChIPseq (46) to define the heterochromatic regions. In wild-type ring- and schizont-stage parasites, Pf H2A.Zac and Pf H2B.Zac were enriched in euchromatin and largely excluded from the H3K9me3-enriched heterochromatin (Fig. 2A). Pf H2A.Zac and Pf H2B.Zac were primarily enriched in intergenic regions (Fig. 2B), consistent with the known occupancy pattern of total Pf H2A.Z and Pf H2B.Z (7–10). The intergenic enrichment was predominantly upstream of genes and was positively correlated with the level of gene expression (Fig. 2B), as previously observed for Pf H2A.Z (47). Interestingly, total and acetylated Pf H2A.Z and Pf H2B.Z were also more enriched in the coding sequence of silent euchromatic genes relative to the coding sequence of expressed euchromatic genes (Fig. 2B), similar to *Toxoplasma gondii* (48).

### Acetylated Pf H2A.Z and Pf H2B.Z are dynamically enriched at active gene promoters

Upstream enrichment patterns of Pf H2A.Z and Pf H2B.Z were positively correlated with transcript levels (Fig. 2), but they were not dynamically associated with gene expression throughout the asexual intra-erythrocytic lifecycle in previous studies (7–10). This indicated that the alternative histones help define the strength of promoters rather than their temporal regulation (9). However, the upstream levels of acetylated Pf H2A.Z and Pf H2B.Z had a stronger association with gene expression than did total levels of Pf H2A.Z and Pf H2B.Z (Fig. 2B). To investigate whether acetylated alternative histones were dynamically enriched at stage-specific expressed genes, we compared enrichment patterns of total alternative histones and their acetylated forms across the promoters of dynamically regulated genes in ring- and schizont-stage parasites. Matched RNAseq data from the same cultures used for ChIPseq (Fig. S2E) were analyzed to select sets of genes

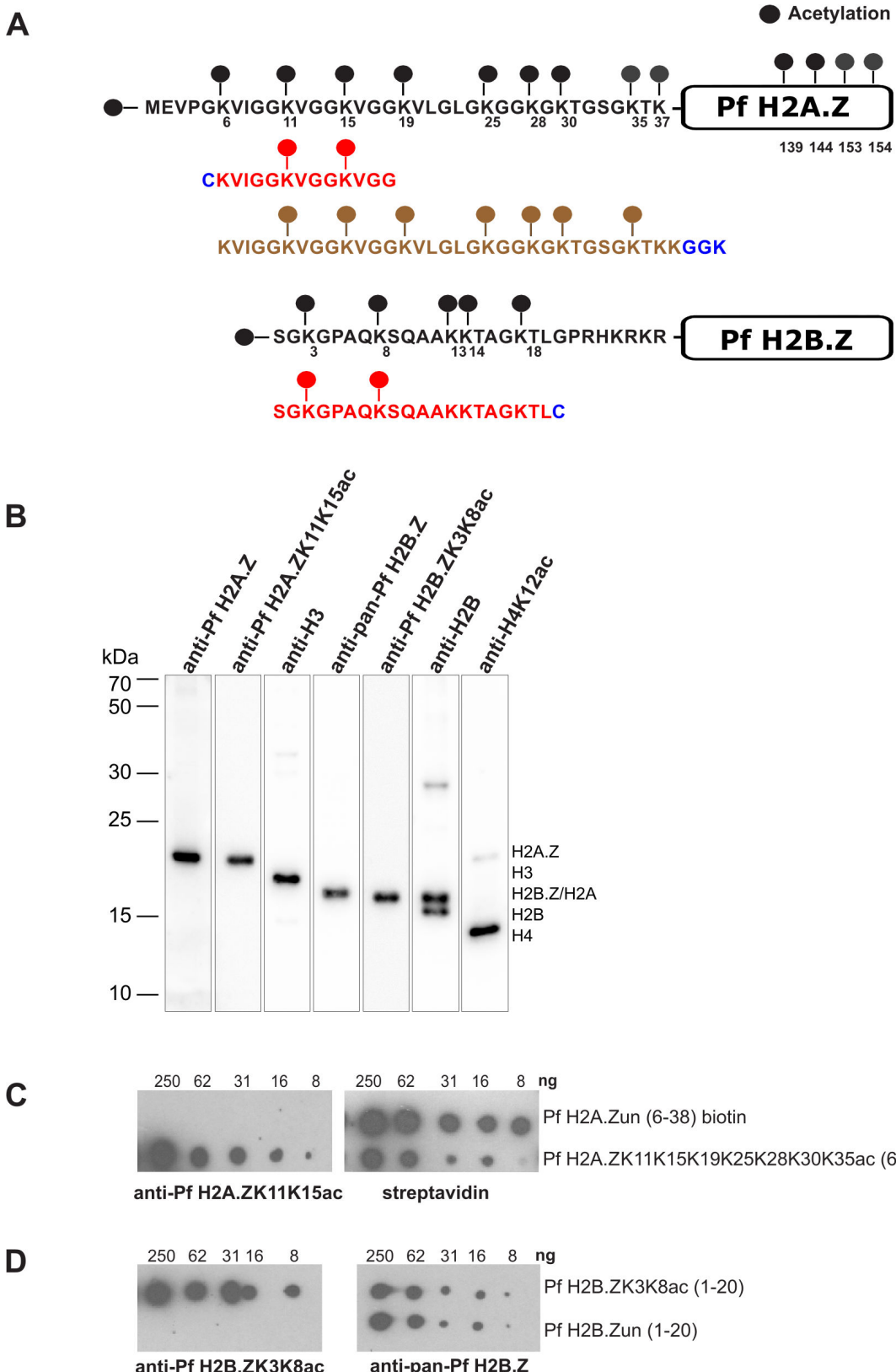


**FIG 1** Validation of antibodies specifically targeting acetylated Pf H2A.Z and Pf H2B.Z. (A) Diagram showing the known acetylations of the N-terminal tails of Pf H2A.Z and Pf H2B.Z with the acetylated peptides used to immunize rabbits in red below and the multi-acetylated biotinylated Pf H2A.Z peptide used for a dot blot in brown. The peptides included terminal cysteine or GGK residues (in blue) for conjugation to keyhole limpet cyanin or biotin, respectively. (B) Western blot showing protein bands for anti-Pf H2A.Z, anti-Pf H2A.ZK11K15ac, anti-H3, anti-pan-Pf H2B.Z, anti-Pf H2B.ZK3K8ac, anti-H2B, and anti-H4K12ac. Lanes are labeled with antibody names and acetylation status. Molecular weight markers (kDa) are on the left. (C) Dot blot analysis of anti-Pf H2A.ZK11K15ac and streptavidin against biotinylated peptides. Lanes are labeled with peptide concentrations (ng). (D) Dot blot analysis of anti-Pf H2B.ZK3K8ac and anti-pan-Pf H2B.Z against biotinylated peptides. Lanes are labeled with peptide concentrations (ng).

**FIG 1 (Continued)**

of parasite extract probed with our previously validated rabbit  $\alpha$ -Pf H2A.Z antiserum (8), affinity-purified  $\alpha$ -H2A.ZK11K15ac antibody,  $\alpha$ -H3 (Abcam, Ab1791),  $\alpha$ -Pf H2B.Z antibody,  $\alpha$ -Pf H2B.ZK3K8ac antibody,  $\alpha$ -H2B antibody (Abcam, Ab1790), and  $\alpha$ -H4K12ac antibody, which cross-reacts with Pf H2A.Z (Millipore, 07-595). (C–D) The unconjugated acetylated and unacetylated peptides were titrated on dot blots and probed with the affinity-purified  $\alpha$ -Pf H2A.Zac or  $\alpha$ -Pf H2B.Zac antibodies and the  $\alpha$ -Pf H2B.Zac pan reactive antibody. (C) Dot blot of titrated biotinylated Pf H2A.Z multi-acetylated peptide and matching unacetylated peptide probed with  $\alpha$ -Pf H2A.ZK11K15ac and streptavidin. (D) Dot blot of titrated unconjugated Pf H2B.ZK3K8ac and matching unacetylated peptide probed with purified Pf H2B.ZK3K8ac antibody and the anti-pan-Pf H2B.Z antibody.

that were in the top quartile by expression in either rings or schizonts and were expressed at least 1.5-fold more in one lifecycle stage than in the other stages (Fig. 3A). The resulting stage-specific gene sets contained 675 genes for ring stage and 392 genes for schizont-stage wild-type parasites (Fig. 3A). Average  $\log_2(\text{ChIP}/\text{input})$  from the concatenated ChIPseq replicates was plotted for the gene sets. There were subtle depletions in 5' intergenic enrichment of total Pf H2A.Z or total Pf H2B.Z in the dynamically expressed gene sets compared to the dynamically repressed gene sets in rings and schizonts (Fig. 3B and C). However, both Pf H2A.Zac and Pf H2B.Zac were clearly dynamically enriched upstream of genes expressed in schizonts (Fig. 3C). In ring stages, Pf H2A.Zac was also clearly dynamically enriched upstream of expressed genes but Pf H2B.Zac was not (Fig. 3B).

To confirm the significance of the dynamic association between acetylated Pf H2A.Z and Pf H2B.Z and gene expression, the 2-kb sequence upstream of the stage-specific gene sets was examined in each ChIP data set to identify the 50-bp window with maximum ChIP/input value, and those maximum values were compared (Fig. 3D). This approach should center on +1 nucleosomes at the transcriptional start site (TSS) rather than diluting the signal from the TSS by averaging enrichment across the 2-kb 5' untranslated region (UTR). For ChIPs of both rings and schizonts, acetylated Pf H2A.Z and acetylated Pf H2B.Z levels were significantly higher upstream of dynamically expressed than dynamically repressed genes (Wilcoxon signed-rank test) (Fig. 3D). Interestingly, in ring stages, the maximum levels of total Pf H2A.Z and total Pf H2B.Z were slightly but significantly lower in dynamically expressed genes than in dynamically repressed genes, and the same trend was evident, although not significant, in schizonts (Fig. 3D). This is consistent with reports from some organisms that H2A.Z was evicted from active gene promoters.

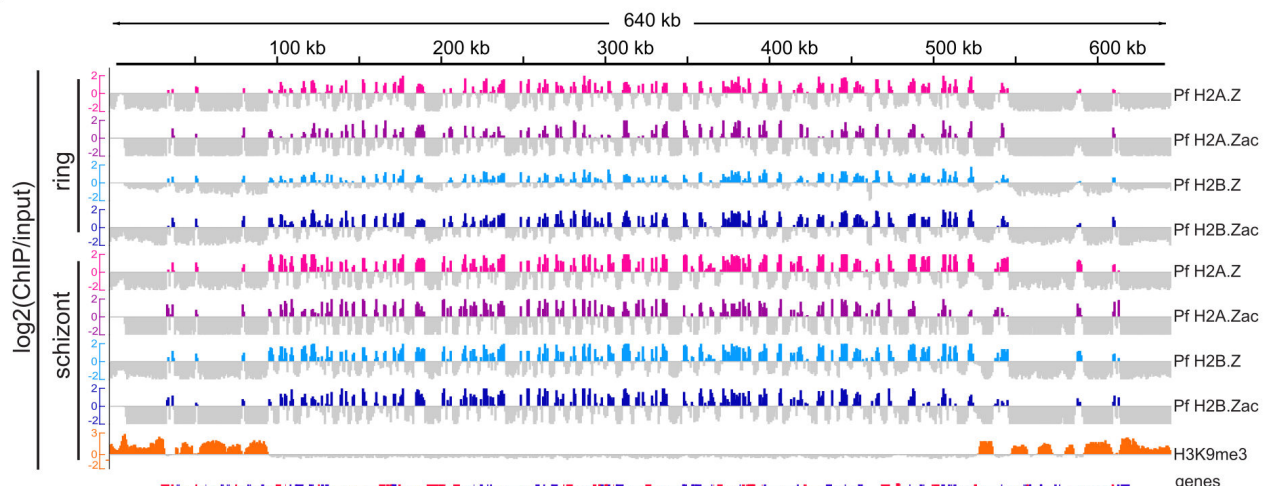
### PfSir2A and PfSir2B antagonize Pf H2A.Z and Pf H2B.Z at chromatin boundaries

Because PfSir2A dynamically antagonizes Pf H2A.Z at active *var* gene promoters (8) and H2A.Z antagonizes telomeric Sir2 in *S. cerevisiae* (42), we next investigated Pf H2A.Z, Pf H2B.Z, and their acetylations in  $\Delta$ PfSir2A and  $\Delta$ PfSir2B parasites (36, 38). Overall, the patterns of enrichment of Pf H2A.Zac and Pf H2B.Zac were similar in the wild-type parasites and the  $\Delta$ PfSir2A or  $\Delta$ PfSir2B parasites (Fig. 4). This is consistent with the predicted function of PfSir2A and B in specifically maintaining heterochromatin (36–38), a region from which Pf H2A.Z and Pf H2B.Z are depleted. To investigate whether more subtle differences in alternative histone enrichment occurred at the euchromatin/heterochromatin boundaries, total or acetylated Pf H2A.Z and Pf H2B.Z ChIPseq peaks were identified by MACS2 (49), and peaks that differed significantly between the wild-type and  $\Delta$ PfSir2A parasites were identified by CSAW (50).

In the  $\Delta$ PfSir2A ring- and schizont-stage parasites, Pf H2A.Z and Pf H2B.Z and their acetylated forms were differentially enriched within heterochromatin as defined by MACS2 called peaks of H3K9me3 in 3D7 ChIPseq (46). They were also enriched in euchromatin adjacent to the boundaries with heterochromatin (Fig. 4; Fig. S3). In the  $\Delta$ PfSir2B parasites, total and acetylated Pf H2A.Z and Pf H2B.Z appeared more enriched in telomeric and subtelomeric heterochromatin regions (Fig. 4; Fig. S3).

To test whether Pf H2A.Z and Pf H2B.Z and their acetylated forms were indeed selectively enriched at the heterochromatin-euchromatin boundaries in  $\Delta$ PfSir2A and

A



B

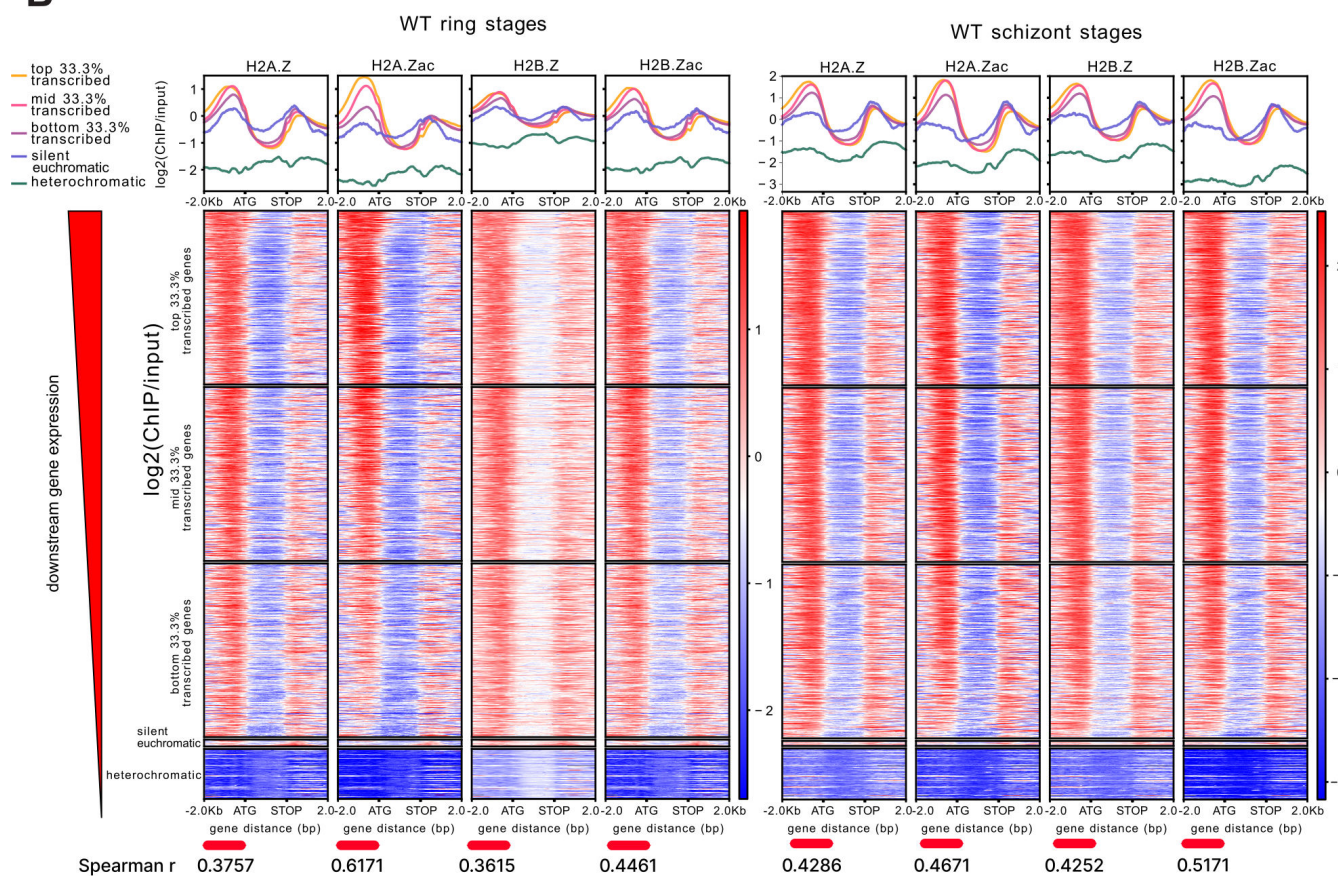


**FIG 2** Alternative histones and their acetylated forms are enriched in upstream, intergenic sequence. (A) Log<sub>2</sub>(ChIP/input) of Pf H2A.Z, Pf H2B.Z, and their acetylated forms plotted across chromosome 1 for chondroitin sulfate A selected 3C ring- and schizont-stage parasites. H3K9me3 in parental 3D7 schizont stages is included as a marker of heterochromatin. (B) Average profile plots and corresponding heatmaps of log<sub>2</sub>(ChIP/input) for the alternative histones and their acetylated forms in 3C ring- and schizont-stage parasites plotted from 2 kb upstream to 2 kb downstream of all *P. falciparum* genes in descending order of expression level [fragments per kilobase of exon per million reads (FPKM)]. Genes were grouped into the five groups of heterochromatic genes; silent euchromatic genes (0 FPKM); and top, mid, and bottom terciles of expressed euchromatic genes. The Spearman *r* correlation between the log<sub>2</sub>(ChIP/input) within the 2-kb region upstream of a gene and the gene's expression (FPKM) is shown under each heatmap (all  $P < 2 \times 10^{-152}$ ).

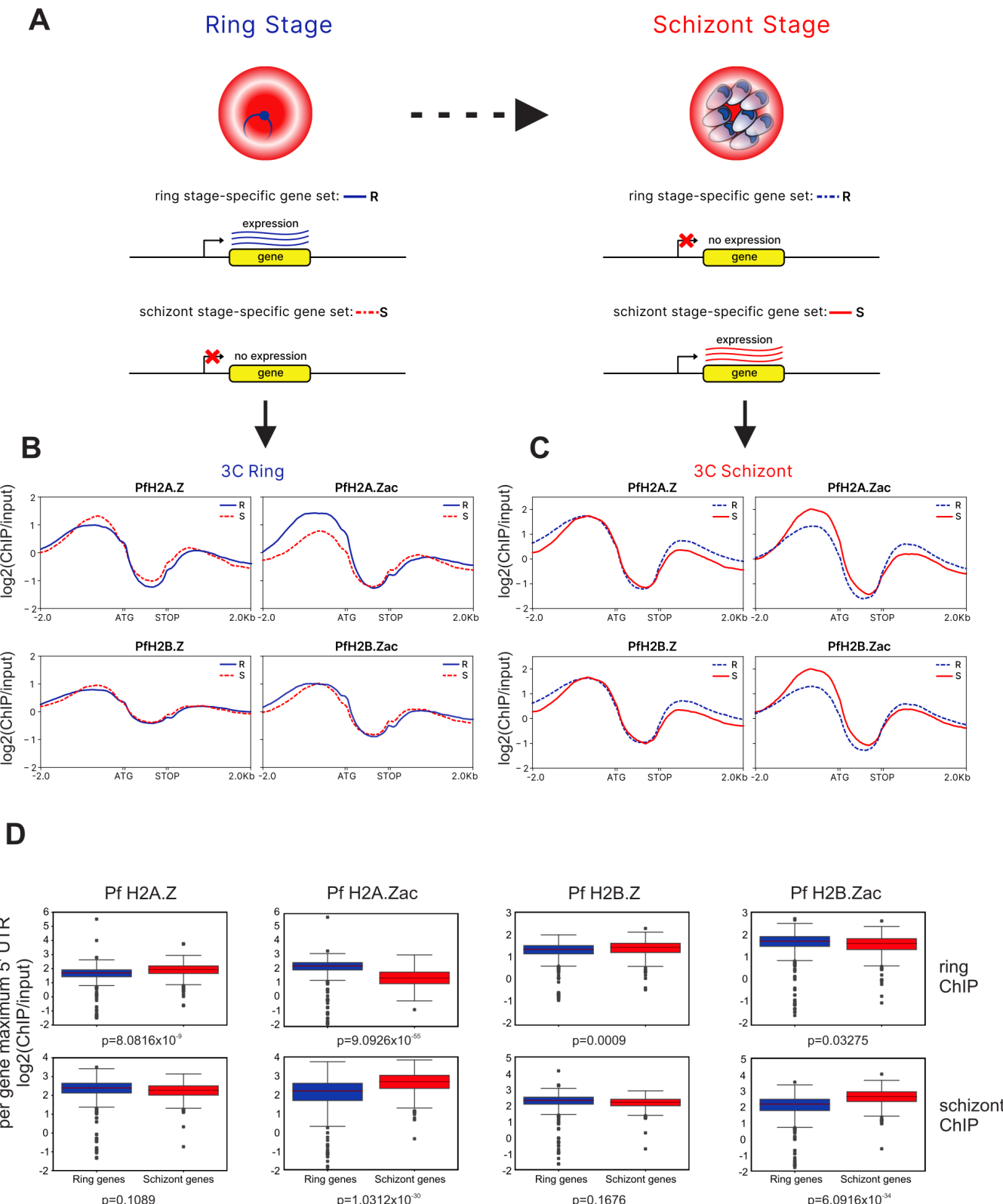


**FIG 3** Pf H2A.Z and Pf H2B.Z are dynamically enriched at promoters of expressed genes. (A) Strategy for selecting stage-specific expressed gene sets that were in the top quartile of expression in a stage and were expressed at least 1.5-fold higher in that stage than the other stage. (B, C)  $\log_2(\text{ChIP}/\text{input})$  average profiles of ring (blue) or schizont (red) stage-expressed gene sets from (B) ring- and (C) schizont-stage ChIPs of wild-type parasites [ring-stage-expressed gene set ( $n = 675$ ) and schizont-stage-expressed gene set ( $n = 392$ )]. Within a stage, the upregulated gene sets are solid lines, and the downregulated gene sets are dashed lines.

**FIG 3 (Continued)**

(D)  $\text{Log}_2(\text{ChIP}/\text{input})$  maximum values for 50 bp windows across 2 kb upstream of genes compared between the same ring and schizont dynamically expressed genes sets from (B and C) for each total and acetylated alternative histone ChIP,  $P$  values Wilcoxon signed-rank test.

$\Delta\text{PfSir2B}$  compared to wild-type parasites, we defined the entire H3K9me3 broad peaks called from 3D7 ChIPseq (46) as 109 ring-stage and 100 schizont-stage heterochromatic test regions. In addition, 138 ring-stage and 131 schizont-stage non-overlapping, flank test regions, each of up to 10 kb of sequence that flanked the H3K9me3 peaks were also identified. Randomly selected size- and chromosome-matched control sequences were selected for each test sequence from the genome masked for the test sequences. Flank and peak read counts were normalized as reads per kilobase per million reads (RPKM), and the average ratio of ChIP/input for two replicates was compared between wild-type and  $\Delta\text{PfSir2A}$  (Fig. 5) or  $\Delta\text{PfSir2B}$  parasites (Fig. S4). In both, rings and schizonts, there were significantly higher levels of Pf H2A.Z, Pf H2A.Zac, and Pf H2B.Zac in the heterochromatin and flanking sequences in the  $\Delta\text{PfSir2A}$  and  $\Delta\text{PfSir2B}$  parasites compared to wild-type parasites (Wilcoxon matched-pairs signed-rank test all  $P < 0.0001$ ) (Fig. 5; Fig. S5). The median values for control sequences were visually indistinguishable between wild-type and  $\Delta\text{PfSir2A}$  or  $\Delta\text{PfSir2B}$  parasites, but in ring stages, the levels of Pf H2B.Zac and Pf H2A.Z in controls trended in the opposite direction to the tests and were actually slightly less in the  $\Delta\text{PfSir2A}$  or  $\Delta\text{PfSir2B}$  parasites compared to wild-type parasites ( $P \leq 0.0407$ ) (Fig. 5; Fig. S4).

In schizonts, Pf H2B.Z also increased in heterochromatin and flanking regions in  $\Delta\text{PfSir2A}$  and  $\Delta\text{PfSir2B}$  parasites compared to wild-type parasites (Fig. 5; Fig. S4). In ring stages, the levels of Pf H2B.Z decreased in heterochromatin in both  $\Delta\text{PfSir2A}$  and  $\Delta\text{PfSir2B}$  parasites compared to wild-type parasites but increased in euchromatic flanking regions in  $\Delta\text{PfSir2A}$  ( $P < 0.0001$ ) but not  $\Delta\text{PfSir2B}$  parasites compared to wild-type parasites. The control flanking regions in rings also had a modest increase in Pf H2B.Z levels in  $\Delta\text{PfSir2A}$  compared to wild type ( $P = 0.0281$ ), preventing any clear inference of an association between PfSir2A and the deposition of Pf H2B.Z in and around heterochromatin in ring-stage parasites. Overall, however, we concluded that Pf H2A.Z, Pf H2A.Zac, Pf H2B.Z, and Pf H2B.Zac were antagonized in heterochromatin and at heterochromatin boundaries by the histone deacetylases PfSir2A and PfSir2B.

#### Acetylated Pf H2A.Z and Pf H2B.Z are enriched downstream of ups B var genes

Pf H2A.Z and Pf H2B.Z are typically depleted at silent members of the heterochromatic *var* multigene family (8, 10), but there was a striking enrichment of total and acetylated alternative histones in the intergenic regions downstream of upsB *var* genes that was not associated with their expression (Fig. 6A and B; Fig. S5). UpsB *var* genes are the most telomeric *var* genes and are transcribed toward the centromere (Fig. 6C); thus the enrichment of acetylated canonical and alternative histone lies between the central chromosome body and the upsB *var* gene/telomere (Fig. 6C). This suggests the acetylated histones could play a structural role at this location, possibly contributing to the barrier against the spread of telomeric heterochromatin into the chromosome bodies.

#### Pf H2A.Z and Pf H2B.Z are acetylated when present at *var* promoters in rings

Unlike most other genes, the levels of total Pf H2A.Z and Pf H2B.Z at *var* gene promoters are dynamically associated with *var* gene expression (8, 10). The histone deacetylase PfSir2A represses *var* genes and antagonizes Pf H2A.Z at *var* gene promoters (8, 36). To investigate the role of PfSir2A in the unique dynamics of Pf H2A.Z and Pf H2B.Z at *var* gene promoters, we assessed the histones' acetylation at the promoters of *var* genes that were derepressed in ring-stage  $\Delta\text{PfSir2A}$  parasites (Fig. 6A). The levels of total and acetylated Pf H2A.Z and Pf H2B.Z were more highly correlated at *var* gene promoters (all *var* 2-kb 5' untranslated regions) (Spearman  $r = 0.97$ ) than throughout the genome (Fig.

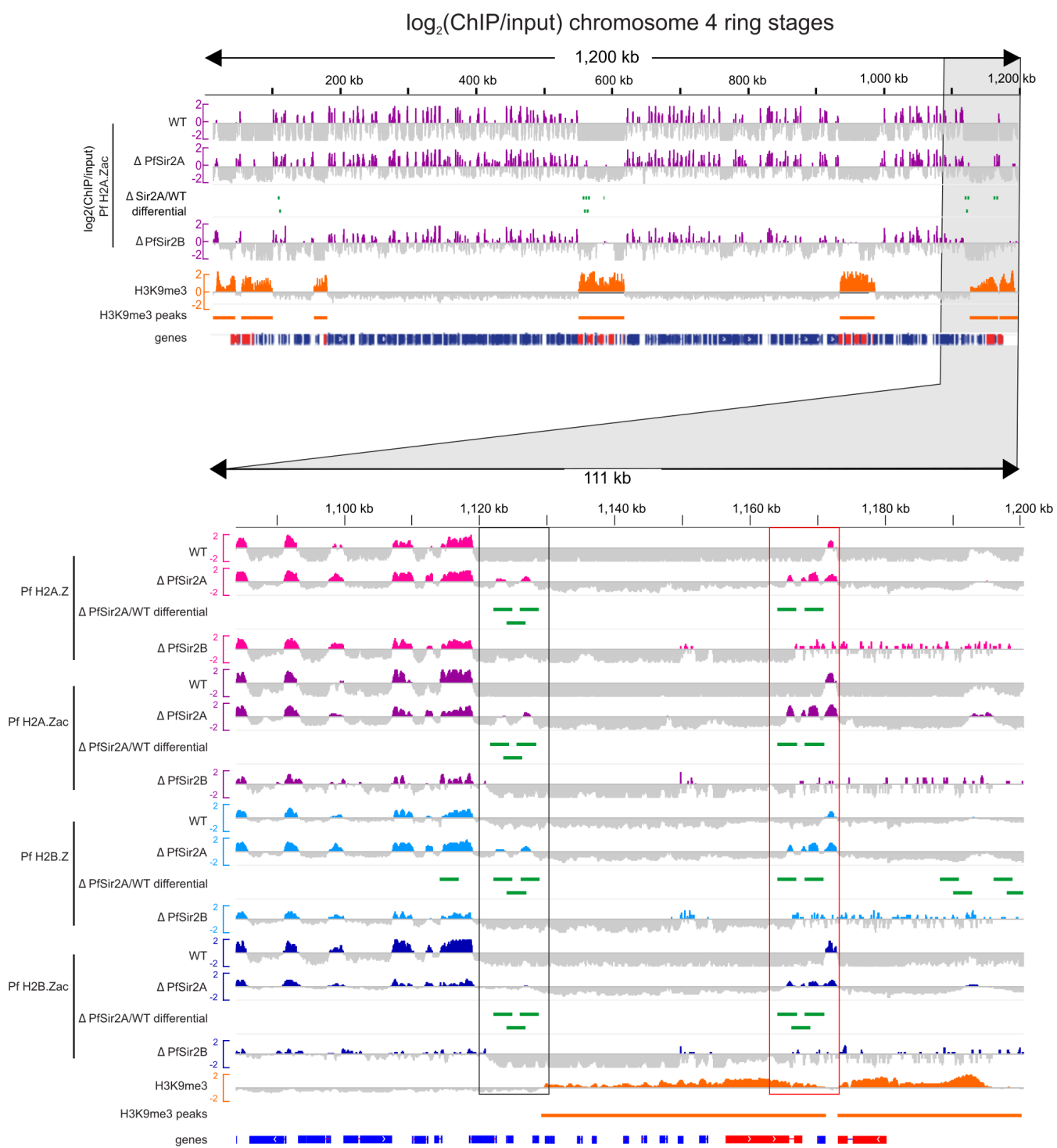


**FIG 4** Total and acetylated Pf H2A.Z and Pf H2B.Z are differentially enriched in heterochromatin in  $\Delta\text{PfSir2A}$  and  $\Delta\text{PfSir2B}$  parasites compared to wild-type (WT) ring stages. A projection of chromosome 4 in ring-stage wild-type 3C,  $\Delta\text{PfSir2A}$ , and  $\Delta\text{PfSir2B}$  parasites showing Pf H2A.Zac  $\log_2(\text{ChIP}/\text{input})$  levels (purple); peaks of Pf H2A.Zac identified as differentially enriched in  $\Delta\text{PfSir2A}$  compared to wild type ( $\Delta\text{PfSir2A}/\text{WT}$  differential, green); ring-stage  $\log_2(\text{ChIP}/\text{input})$  H3K9me3 (orange); and peaks of H3K9me3 in wild-type 3D7 (orange lines). Genes are indicated in blue, with var genes superimposed in red. The lower panel zooms into 111 kb from the right-hand end of chromosome 4 and shows the data as above but also for total and acetylated Pf H2A.Z and Pf H2B.Z with boxed regions indicating regions of differential enrichment of total and acetylated histones between wild-type and  $\Delta\text{PfSir2A}$  parasites at the euchromatin/heterochromatin boundary (black box) and downstream of upsB var genes within subtelomeric heterochromatin domains (red box).

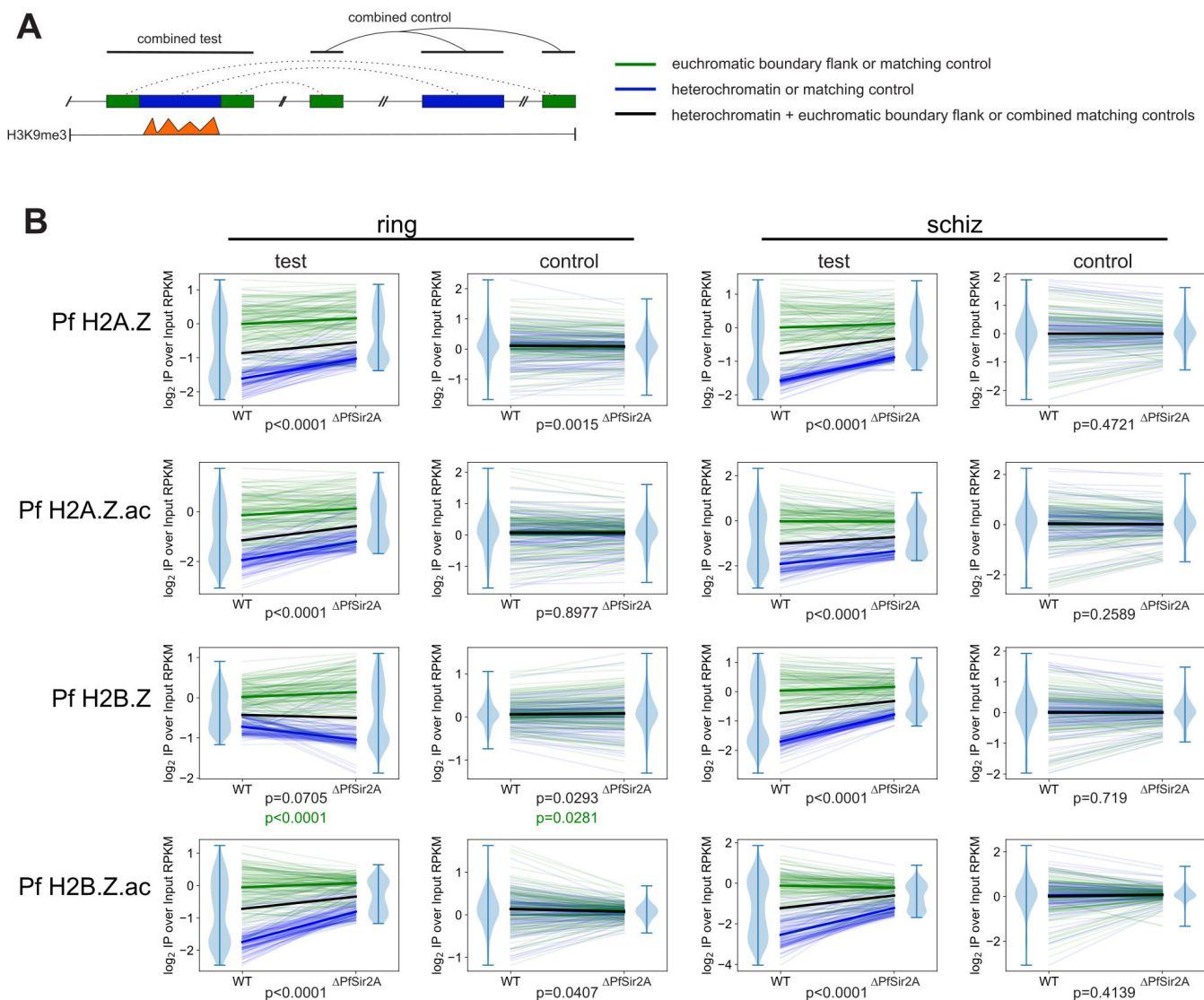


**FIG 5** Total and acetylated Pf H2A.Z and Pf H2B.Z are antagonized by PfSir2A at heterochromatin boundaries. (A) Model of scheme for selecting test and control regions for comparison between wild-type (WT) and  $\Delta$ PfSir2A parasites. The compared regions were 109 ring-stage and 100 schizont-stage heterochromatic test regions defined by H3K9me3 broad peaks called from 3D7 ChIPseq (blue) (46) and 138 ring-stage and 131 schizont-stage non-overlapping, flank test regions, each of up to 10 kb of sequence (green). Size- and chromosome-matched control sequences were randomly selected (dotted lines) for each test sequence and are color coded the same. (B) Average ratios of  $\log_2(\text{ChIP}/\text{input})$  for two replicates of total and acetylated Pf H2A.Z and Pf H2B.Z ChIP normalized as RPKM compared between wild-type and  $\Delta$ PfSir2A parasites. Medians for heterochromatin and matched controls (blue) or flanks and matched controls (green) are shown in thick, bold lines, and medians for the combined heterochromatin and flank test regions or their matching controls are shown in thick black bold. *P* values are for Wilcoxon matched-pairs signed-rank test comparisons between wild-type and  $\Delta$ PfSir2A parasites of combined heterochromatin and flank test regions or their matching controls (in black) or flanking regions only (in green for Pf H2B.Z). Violin plots at the edges of line plots indicate the frequency distribution of the combined heterochromatin and flank regions or matching control regions, and bars indicate the range.

S2) (Spearman  $r \leq 0.79$ ), suggesting that most of the Pf H2A.Z and Pf H2B.Z present at the derepressed *var* promoters were acetylated. This implicates PfSir2A deacetylase activity in Pf H2A.Z and Pf H2B.Z dynamics at *var* gene promoters.

#### Var gene intron promoter activity is associated with enrichment of acetylated Pf H2A.Z and Pf H2B.Z

*Var* gene introns have promoter activity that has been previously associated with *var* gene silencing (40, 51). Schizont stage parasites express sterile *var* exon 2 transcripts

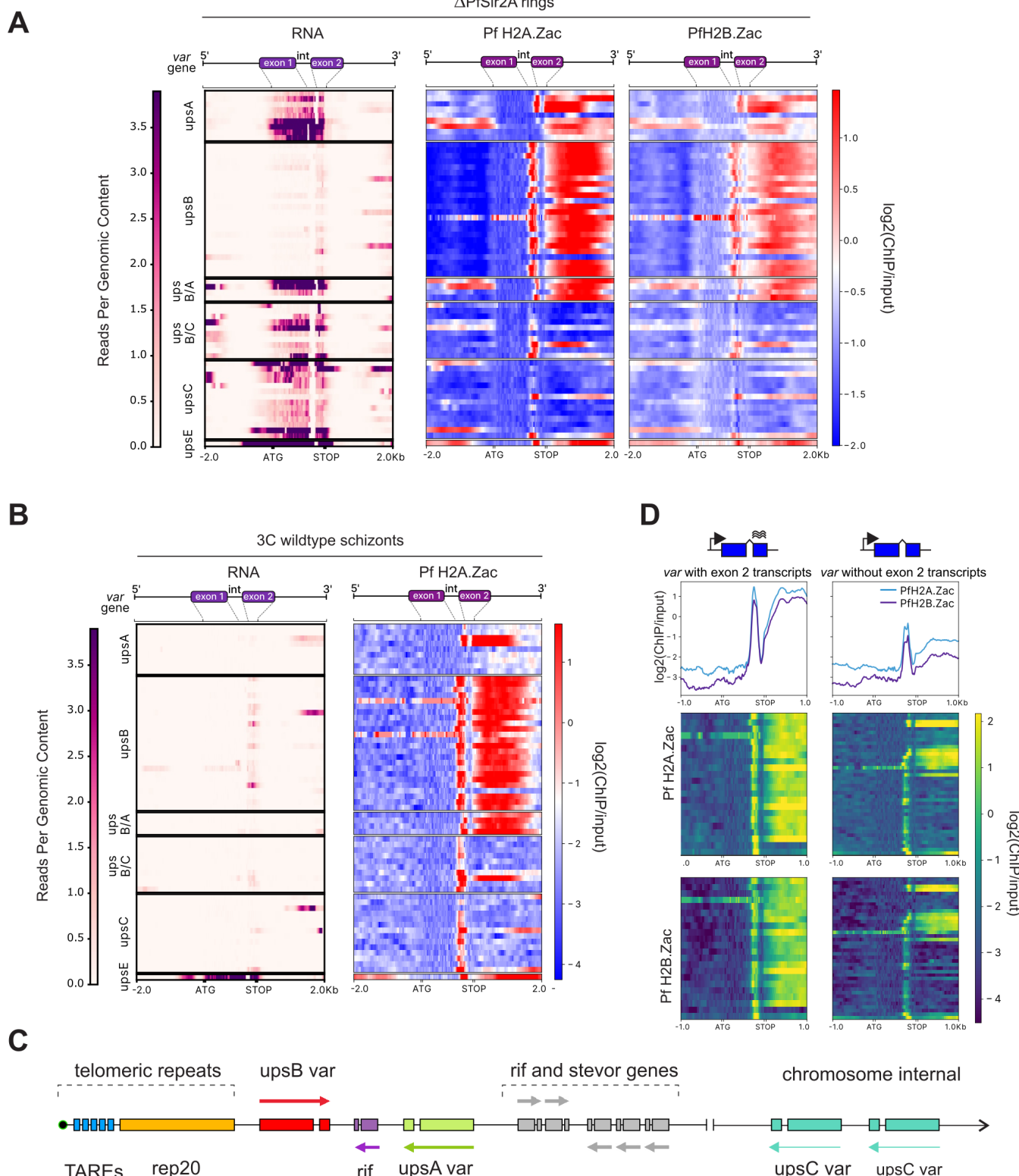


**FIG 6** Pf H2A.Zac and Pf H2B.Zac are enriched at transcribed *var* gene promoters and *var* introns. RNAseq reads per genomic content and  $\log_2(\text{ChIP}/\text{input})$  for Pf H2A.Zac and Pf H2B.Zac plotted from 2 kb upstream to 2 kb downstream of the genomic repertoire of 65 *var* genes in (A) ring-stage  $\Delta\text{PfSir2A}$  parasites and (B) schizont-stage wild-type parasites. The heatmaps are scaled to render all *var* genes the same length; therefore, the gene diagrams at the top of the heatmaps only approximate the intron-exon boundaries (int, intron). (C) Diagram illustrating the genomic arrangement of *var* genes in subtelomeric and chromosome internal heterochromatin. (D)  $\log_2(\text{ChIP}/\text{input})$  of Pf H2A.Zac and Pf H2B.Zac across *var* genes that did or did not transcribe the exon 2 in schizont-stage wild-type parasites. TAREs = telomere associated repeat elements.

driven by the intron promoters, primarily from *upsB var* genes (Fig. 6B and C). The presence of acetylated Pf H2A.Z and Pf H2B.Z was associated with the level of expression of sterile *var* exon 2 transcripts in schizonts (Fig. 6D; Fig. S5). This suggested that acetylated Pf H2A.Z and Pf H2B.Z also contributed to regulating *var* intron promoter activity.

### Pf H2A.Zac and Pf H2B.Zac are deacetylated by class I and II histone deacetylases

PfSir2A could potentially deacetylate Pf H2A.Z and Pf H2B.Z but only within heterochromatin and at heterochromatin boundaries (Fig. 4 and 5). Some other enzymes must therefore be responsible for the dynamic deacetylation of the bulk of Pf H2A.Zac and Pf H2B.Zac at euchromatic genes when their expression decreases. *P. falciparum* has five HDACs, the class I PfHDAC1, the class II PfHDAC2 and PfHDAC3, and the class III sirtuins, PfSir2A and PfSir2B. To investigate whether class I or II HDACs can also deacetylate Pf H2A.Zac and Pf H2B.Zac, we tested the pan-class I and II HDAC inhibitors apicidin and trichostatin A (52, 53). Treatment of parasites with both inhibitors increased the amount of acetylated Pf H2A.Z and Pf H2B.Z (Fig. S6). This suggests that the bulk of Pf H2A.Zac and Pf H2B.Zac within euchromatin is deacetylated by class I or II HDACs.

## DISCUSSION

Total and acetylated Pf H2A.Z and Pf H2B.Z have highly correlated distributions in both ring- and schizont-stage parasites (Fig. S2), suggesting that the majority of Pf H2A.Z and Pf H2B.Z are acetylated to some extent in asexual blood stage *P. falciparum*. However, upstream of genes, the levels of acetylated Pf H2A.Z and Pf H2B.Z are dynamically and positively associated with the genes' expression. The role of H2A.Z at promoters is enigmatic, it functions differently depending on species, chromatin context, and genes studied (54). In human cells, different patterns of H2A.Z enrichment in promoters had different effects on gene expression (16). A well-positioned, micrococcal nuclease-sensitive, i.e., relatively unstable, H2A.Z-containing nucleosome at the TSS was associated with highly expressed genes, and poorly positioned, dispersed H2A.Z-containing nucleosomes were associated with gene repression. *P. falciparum* has poorly positioned nucleosomes across its promoters consistent with the slight, negative association between dynamic gene expression and total Pf H2A.Z and Pf H2B.Z enrichment in ring stages. However, there is a well-positioned nucleosome at the TSS which is frequently evicted when *P. falciparum* genes are expressed (55), consistent with the presence of an unstable nucleosome containing acetylated Pf H2A.Z.

The dynamic enrichment of acetylated Pf H2A.Z and Pf H2B.Z at active promoters could function to drive transcription through biophysical alteration of chromatin. Nucleosomes at the +1 site can block RNA PolII progression, but H2A.Z at the +1 nucleosome is important in preventing stalling of RNA PolII, suggesting that H2A.Z plays an important role in elongation, possibly through destabilizing the nucleosomes at the +1 position (56). Homotypic H2A.Z-H2A.Z nucleosomes are less stable than H2A-containing nucleosomes (57) and are enriched immediately downstream of the TSS of active genes at the +1 position (58). The only detectable Pf H2A.Z nucleosomes are homotypic (10) so are presumably less stable than H2A-containing nucleosomes. Mechanistically, the flexible DNA ends of nucleosomes containing H2A.Z reduce their stability compared to H2A-containing nucleosomes (15). Acetylation of H2A.Z reduces nucleosome stability further (17) and has been associated with promoter activity in other species (19, 23). Thus, the enrichment of acetylated Pf H2A.Z and Pf H2B.Z at promoters could destabilize nucleosomes to create chromatin that is permissive for transcription. The slightly decreased levels of total Pf H2A.Z and Pf H2B.Z upstream of dynamically expressed genes suggest that the increased levels of Pf H2A.Z and Pf H2B.Z acetylation destabilize the nucleosomes leading to their increased eviction at active gene promoters, similar to yeast and metazoans (19–24). The mechanism of H2A.Z eviction remains

unclear. Both the PIC (25) and the ATP-dependent chromatin remodeler INO80 have been implicated (26), although *P. falciparum* possesses no annotated orthologs of INO80 (PlasmoDB).

Acetylated H2A.Z may recruit other factors which affect chromatin function. Pf H2A.Z co-localizes with the bromodomain protein PfBDP1 at nucleosome-depleted regions that bind the transcription factor AP2-I in expressed invasion gene promoters (11), and PfBDP1 binds acetylated Pf H2A.Z and Pf H2B.Z peptides (32), suggesting that Pf H2A.Zac may directly recruit bromodomain protein containing transcriptional complexes. Acetylated Pf H2A.Z/ Pf H2B.Z might also interact with other histone modifications and histone modifiers to affect gene expression. Incorporation of H3.3 destabilizes H2A.Z-containing nucleosomes at promoters and enhancers of active genes in vertebrates (59, 60), and Pf H3.3 is also enriched at active *var* gene promoters along with Pf H2B.Z and Pf H2A.Z (8, 10, 61). However, it does not appear to be a genome-wide mechanism for coordinating gene expression because Pf H3.3 enrichment at promoters genome wide does not correlate with *P. falciparum* gene expression (61).

*P. falciparum* relies on variegated expression of contingency genes as a bet-hedging strategy for environmental adaptation (62). These contingency genes are localized to clusters of loci in facultative heterochromatin at subtelomeric and a few chromosome-internal sites. A limited number of these genes escape gene silencing and are expressed within the discontinuous stretches of facultative heterochromatin, with random switching between expressed members of multi-gene families conferring variant phenotypes on clonal progeny (62). Maintenance of a dynamic heterochromatin boundary is clearly critical to this process. In *S. cerevisiae*, H2A.Z antagonizes both the spread of Sir2-mediated silencing (42) and silencing of genes by the global sirtuin deacetylase Hst3, possibly through forming a localized barrier at promoters to Hst3 silencing activity (44). We have now shown that PfSir2A antagonizes the spread of total and acetylated Pf H2A.Z and Pf H2B.Z in an analogous process suggesting a role for H2A.Z as a heterochromatin barrier that is conserved across diverse taxa.

The best studied of the *P. falciparum* heterochromatic contingency genes is the *var* multigene family, a single member of which escapes silencing and is expressed in ring-stage parasites. We had previously shown that unlike other genes, silent *var* gene promoters were depleted of total Pf H2A.Z and Pf H2B.Z in wild-type *P. falciparum*. However, in  $\Delta$ PfSir2A parasites, multiple *var* genes are de-repressed, and Pf H2A.Z and Pf H2B.Z are enriched at their promoters (8, 36). Here, we show that Pf H2A.Z and Pf H2B.Z at these *var* promoters are acetylated. PfSir2A could directly deacetylate the small fraction of total Pf H2A.Z and Pf H2B.Z that are present at heterochromatin barriers and *var* promoters. Alternatively, PfSir2A could indirectly antagonize Pf H2A.Z/Pf H2B.Z and their acetylation through deacetylating other histones. In *S. cerevisiae*, the Swr1 complex is stably bound to heterochromatin boundaries and is induced to deposit H2A.Z/H2B dimers in promoter nucleosomes by the NuA4 histone acetyltransferase complex acetylating H4. Thus, acetylated H4 and H2A.Z coordinate to activate genes in these regions (43). *P. falciparum* has a Swr1 ortholog, so PfSir2A could indirectly antagonize acetylated Pf H2A.Z and Pf H2B.Z by deacetylating H4 (63) and blocking Pf H2A.Z and Pf H2B.Z deposition by Swr1. In *S. cerevisiae*, the histone acetyltransferase GCN5 can acetylate H2A.Z (64), and the *P. falciparum* GCN5 bromodomain binds acetylated H4 (32). Consequently, by blocking PfGCN5 binding to H4ac sirtuins could also indirectly antagonize Pf H2A.Z and Pf H2B.Z acetylation.

We observed strong enrichment of acetylated Pf H2A.Z and Pf H2B.Z in *var* gene introns, which was associated with the introns' promoter activity and exon 2 expression levels. Similarly, enrichment of homotypic H2A.Z nucleosomes at intron-exon boundaries in *Drosophila* was associated with gene expression and was proposed to be a consequence of the transcriptional machinery encountering regions of differing nucleosomal density (58). The enrichment at *var* intron boundaries could also possibly reflect a sequence preference for Pf H2A.Z- and Pf H2B.Z-containing nucleosomes as the *var*

intron boundaries have a unique sequence composition and are enriched in complementary repeat sequences (65).

The differential enrichment of acetylated Pf H2A.Z and Pf H2B.Z in heterochromatin in  $\Delta$ PfSir2A parasites was often in the downstream sequences between convergent upsA and upsB var genes (Fig. 4 and 6; Fig. S3), suggesting the enrichment in this region was antagonized by PfSir2A. UpsB var genes are frequently the first coding sequence after non-coding subtelomeric repeats, so the enrichment of acetylated Pf H2A.Z and Pf H2B.Z in the var introns and downstream of the upsB var genes could play a fundamental role in containing the spread of silent, telomeric heterochromatin, rather than in var gene regulation *per se*. Alternatively, as the regions between upsA and upsB var genes are also enriched in other small contingency gene family members, e.g., rif, the enrichment of acetylated alternative histones here may relate to the variegated expression of members of these gene families.

In conclusion, the acetylated and total *P. falciparum* alternative histones Pf H2A.Z and Pf H2B.Z co-localize across the genome, suggesting that the majority of Pf H2A.Z and Pf H2B.Z are acetylated. However, their acetylation at gene promoters is dynamically associated with expression of stage-specific genes and var genes. These observations suggest they play an important role in marking promoters and in promoter activation. Acetylated Pf H2A.Z and Pf H2B.Z are also antagonized by PfSir2A and PfSir2B at heterochromatin boundaries, indicating they additionally are involved in maintaining proper chromatin structure in *P. falciparum*. Finally, they are enriched in var gene introns and downstream of mainly upsB var genes independent of var gene expression, suggesting they play a structural role in maintaining the chromatin compartments of *P. falciparum*.

## MATERIALS AND METHODS

### Parasites

The cloned PfSir2A and PfSir2B knockout made in a *P. falciparum* 3D7 clone background were previously described (36, 38) as was the wild-type 3C subpopulation of the *P. falciparum* 3D7 clone that was selected for predominantly var2csa expression by panning on purified chondroitin sulfate A (66). Parasite cultures were maintained as previously described (11) and regularly synchronized using 5% sorbitol.

### Histone Western blot

Pellets from 3D7 parasite cultures were lysed in 0.15% saponin in PBS, and the parasite pellets were extracted in 2× Laemmli buffer. Parasite extracts were loaded onto 12% BisTris gels (Invitrogen) and separated in 1× MES running buffer (Invitrogen). After transferring the proteins onto nitrocellulose membranes and blocking with 5% milk in Tris-buffered saline-Tween (TBS-T), the blot was cut into strips, and each strip was incubated with different antibodies overnight at a dilution of 1:2,000. After washing and incubation with horse radish peroxidase (HRP)-coupled goat anti-rabbit antibodies (Invitrogen), the strips were developed with Immobilon ECL reagent (Millipore). As all strips were derived from the same membrane, alignment of the strips facilitated accurate size determination of the detected histones and histone variants. Rabbit antibodies were anti-H3 (Abcam, Ab1790), anti-H4K12ac (Millipore 07-595), anti-H2B (Abcam, Ab1790). Images were acquired in the optimal dynamic range using the Vilber Fusion FX system.

### Dot blot

The peptides analyzed were the acetylated and non-acetylated version of the Pf H2A.Z and Pf H2B.Z peptides used for immunization (Fig. 1A) and H3K9ac ARTKQ-TARK(Ac)STAGKAPRKQLAGGK(Biot), H3K18ac ARTKQTARKSTAGKAPRK(Ac)QLAGGK(Biotin), H3K9K14K18ac ARTKQTARK(Ac)STAGK(Ac)APRK(Ac)QLAGGK(Biotin), H3K27ac ASKAARK(Ac)SAPISAGIKKPHRYRPGGK(Biot), H3K23K27ac

ASK(Ac)AARK(Ac)SAPISAGIKKPHRYRPGGK(Biot), H3K56ac ALREIR-  
 RYQK(Ac)STDLLIRKLGGK(Biot), H4K5K8K12K16ac SGRG-K(Ac)-GG-  
 K(Ac)-GLG-K(Ac)-GGA-K(Ac)-RHRKVLRDNGSGS-K(Biot), H4K8ac  
 SGRGKGG-K(Ac)-GLGKGGAKRHRKV-GGK(Biot), H4K16ac SGRGKGGKGLGKGGA-K(Ac)-  
 RHRKVGG-K(Biot), H4K12ac SGRGKGGKGLG-K(Ac)-GGAKRHRKVGG-K(Biot), and H4  
 SGRGAGGAGLGAGGAARHRKVLRDNGSGS-K(biotin). One microliter of peptides (200, 40,  
 8, and 1.6 ng) was spotted onto nitrocellulose membrane and air dried prior to blocking  
 in Tris-buffered saline pH 7.5 0.05% Tween 20 and 5% (wt/vol) skim milk powder for at  
 least 1 hour. For detection with antibodies, the membranes were then incubated overnight  
 at 4°C with primary antibody in 5% skim milk in TBS-T  $\alpha$ -Pf H2A.Zac 2  $\mu$ g,  $\alpha$ -Pf H2B.Zac  
 4  $\mu$ g with rocking overnight. The next day, the membranes were washed three times in  
 TBS-T for 15 minutes each at room temperature, incubated again with 5% skim milk in  
 TBS-T for 30 minutes and then with 1/20,000 diluted goat  $\alpha$ -rabbit-HRP (Invitrogen) in  
 5% skim milk in TBS-T, then washed three times for 20 minutes each in TBS-T, and then  
 incubated for several minutes with Clarity enhanced chemiluminescence (ECL) reagents  
 (Biorad) prior to imaging. For detection of biotinylated peptides, the blocked membrane  
 was washed eight times for 10 minutes each in TBS-T, then incubated at room temperature  
 for 30 minutes with 1/50,000 diluted streptavidin-HRP (Abcam) in TBS-T with rocking. The  
 membrane was washed three times for 20 minutes each with TBS-T at 4°C with rocking  
 prior to development with ECL reagent. For total peptide detection, an unblocked dot blot  
 was incubated with 0.1% (wt/vol) Ponceau S in 5% acetic acid for 5 minutes and destained  
 in water.

### HDAC inhibitor assay

Wild-type parasite cultures were tightly synchronized and seeded in triplicates into six-well plates at 7% ring-stage parasitemia. Cultures were treated with 200 nM Trichostatin A (TSA) or 70 nM apicidine and equivalent volumes of dimethyl sulfoxide (DMSO) as a control. The cultures were incubated for 4 hours with the inhibitors before red blood cells were lysed with 0.15% saponin in PBS, and parasite pellets were extracted for Western blot (67). Parasite proteins were separated by SDS-PAGE on 4%–12% Bis-Tris gels (Invitrogen) and transferred to nitrocellulose membranes. The membranes were blocked with 5% non-fat milk in TBS-T buffer and incubated overnight with primary antibodies at a dilution of 1:2,000. Secondary goat anti-rabbit HRP antibodies were used at a dilution of 1:20,000.

### Cross-linked chromatin immunoprecipitation

Synchronized PfSir2A-KO and wild-type parasites were harvested at ring stage 16 hours post invasion and at schizont stage 42 hours post invasion and cross-linked chromatin prepared as described previously (8). Sonicated chromatin was diluted 1:10 in ChIP dilution buffer (0.01% SDS, 1.1% Triton X-100, 1.2 mM EDTA, 16.7 mM Tris-HCl pH 8.1, 150 mM NaCl) and mixed with an equal volume of Protein A/Protein G Sepharose beads (GE Healthcare). Antibodies used were rabbit anti-Pf H2A.Z and its preimmune serum (8), and the anti-Pf H2A.Zac, anti-Pf H2B.Zac, and pan-reactive anti-Pf H2B.Z generated by Anaspec in rabbits as described in the Results, rabbit anti-H3K9me3 (Active Motif catalog number 39161), a rabbit IgG polyclonal isotype control (Abcam ab37415) non-specific antibody was used as a negative control for the ChIPs with Anaspec antibodies. Chromatin was immunoprecipitated overnight at 4°C, and then the beads were serially washed for 5 minutes with agitation at 4°C first with 1 mL of low salt immune complex wash buffer (0.1% SDS, 1% Triton X-100, 2 mM EDTA, 20 mM Tris-HCl pH 8.1, 150 mM NaCl), then with high salt immune complex wash buffer (0.1% SDS, 1% Triton X-100, 2 mM EDTA, 20 mM Tris-HCl pH 8.1, 500 mM NaCl), then with LiCl immune complex wash buffer (0.25M LiCl, 1% IGEPAL-630, 1% deoxycholate, 1 mM EDTA, 10 mM Tris-HCl pH 8.1). Beads were then washed twice at room temperature for 5 minutes each with Tris-EDTA buffer (10 mM Tris-HCl pH 8.1, 1 mM EDTA pH 8.0) and then chromatin

eluted by incubating twice with separate 100  $\mu$ L aliquots of freshly made elution buffer (1% SDS, 0.1 M NaHCO<sub>3</sub>) for 15 minutes at room temperature.

### ChIP-seq and RNA-seq library preparation

ChIP DNA samples were quantified with the Qubit dsDNA HS Assay Kit (Q32851) (Invitrogen), and 4 ng of each ChIP DNA was used to make sequencing libraries with the NEBNext Ultra II DNA Library Prep Kit for Illumina (E7645) but using KAPA HiFi PCR kit containing high-fidelity KAPA HiFi DNA polymerase enzyme (Roche) for library amplification (12 cycles of 10 s at 98°C and 1 minute at 65°C).

RNA from ring-stage- and schizont-stage-infected erythrocytes was extracted and used to make Illumina RNAseq libraries as previously described (68) but with the omission of globin mRNA depletion.

ChIP DNA and cDNA libraries were quantitated and checked for adapter ligation by qPCR using P5/P7 primers, and library size, purity, and quality were confirmed with the Agilent High Sensitivity DNA kit and reagents (Agilent) on the automated electrophoresis Agilent 2100 Bioanalyzer system. The 150-bp paired-end libraries were sequenced on the Illumina Novaseq 6000 system at the Victorian Clinical Genetics Services, Murdoch's Children Research Institute, Parkville, Victoria, Australia.

### Sequence pre-processing

Fastq files were checked for quality using FastQC tool (version 0.11.8, <https://www.bioinformatics.babraham.ac.uk/projects/fastqc/>), and adaptor sequences were trimmed with TrimGalore (version 0.4.4, [www.bioinformatics.babraham.ac.uk/projects/trim\\_galore](https://www.bioinformatics.babraham.ac.uk/projects/trim_galore)).

### RNA-seq analysis

Trimmed reads were aligned to the *P. falciparum* 3D7 reference genome (version 34) using STAR (version 2.6.0) (69) and converted to BAM format, sorted, and indexed using SAMtools version 1.9 (70). Gene read counts were determined from BAM files using featureCounts (71) and counts normalized by expressing as fragments per kilobase of exon per million reads mapped (FPKM) or reads per genomic content [reads normalized to 1x sequencing depth where sequencing depth is defined as: (mapped reads x fragment length)/23 Mb genome size]. FPKM values were used to rank genes by expression.

### ChIP-seq analysis

Trimmed reads were aligned to the *P. falciparum* 3D7 reference genome, version 34 (PlasmoDB) using bowtie2 version 2.3.4.3 (72). Alignments were converted to BAM format, sorted, and indexed using SAMtools version 1.9 (70), and the indexed and sorted bam files were converted into bigwig formatted files using the bamcoverage tool with a 50-bp window from the DeepTools suite (73). Peaks of ChIP library reads that were enriched relative to input library reads were called using MACS2 version 2.1.2.1 (49), with the *q*-value threshold parameter of 0.05. Called peaks were visualized with the Integrated Genome Viewer (74). ChIP peaks that were differentially enriched between different ChIP libraries were identified using CSAW (50) with the default false discovery rate of 0.05.

### Analysis of ChIP read counts within boundaries between euchromatin and H3K9me3-enriched heterochromatin

MACS2 (49)-called peaks of H3K9me3/input in 3D7 parasites were used to identify regions of heterochromatin in ring and schizont stages. Read counts were determined using featureCounts (71) for Pf H2A.Z, Pf H2A.Zac, Pf H2B.Z, and Pf H2B.Zac within heterochromatin and for 10 kb of flanking sequence on each side of the heterochromatic regions. In cases where two heterochromatic regions were separated by less than 10 kb, the entire interval between them was used. In cases where flanking sequences completely overlapped, one was randomly chosen for analysis. Of the 100–130 regions

analyzed, eight flanking sequences partially overlapped and were retained. Bedtools shuffle (75) was used to randomly select size-matched control sequences from the same chromosome as the heterochromatic and flanking sequences with heterochromatic and flanking sequences excluded. Heterochromatic and flanking region read-depth was normalized as RPKM, which was converted to a ratio of  $\log_2(\text{ChIP}/\text{input})$  and averaged for the two replicates. The read count ratios were compared between wild-type and *ΔPfSir2A* samples using a Wilcoxon matched-pairs signed-rank test.

## ACKNOWLEDGMENTS

This work was supported by the Australian National Health and Medical Research Council (NHMRC) through project grants GNT1128975 to M.F.D. and GNT1084580 to M.P. This work was further supported by the German Research Foundation (DFG) through project 433302244 to M.P. and by the DFG Research Infrastructure NGS\_CC as part of the Next Generation Sequencing Competence Network (project 423957469).

We also would like to acknowledge Universities Australia and the German Academic Exchange Service (DAAD) for support through the Australia-Germany Exchange Scheme.

## AUTHOR AFFILIATIONS

<sup>1</sup>School of BioSciences, The University of Melbourne, Melbourne, Australia

<sup>2</sup>Bio21 Institute, Parkville, Victoria, Australia

<sup>3</sup>School of Medicine, Faculty of Health, Deakin University, Geelong Waurn Ponds Campus, Waurn Ponds, Australia

<sup>4</sup>Universitätsklinikum Erlangen, Mikrobiologisches Institut – Klinische Mikrobiologie, Immunologie und Hygiene, Friedrich-Alexander-Universität (FAU) Erlangen-Nürnberg, Erlangen, Germany

<sup>5</sup>Harvey Mudd College, Claremont, California, USA

<sup>6</sup>Department of Microbiology and Immunology, Peter Doherty Institute for Infection and Immunity, The University of Melbourne, Melbourne, Victoria, Australia

## PRESENT ADDRESS

Suffian Azizan, Nanyang Technological University, Nanyang Ave, Singapore

Shamista A. Selvarajah, Australia Post Victoria, Victoria, Australia

Jingyi Tang, Diagnostics Collingwood Victoria, Victoria, Australia

## AUTHOR ORCIDs

Suffian Azizan  <http://orcid.org/0000-0001-8991-1422>

Danae Schulz  <http://orcid.org/0000-0002-0392-7245>

Michaela Petter  <http://orcid.org/0000-0002-1837-2756>

Michael F. Duffy  <http://orcid.org/0000-0001-5635-4033>

## FUNDING

Funder	Grant(s)	Author(s)
DHAC   National Health and Medical Research Council (NHMRC)	GN1128975	Michael F. Duffy
DHAC   National Health and Medical Research Council (NHMRC)	GN1084580	Michaela Petter
Deutsche Forschungsgemeinschaft (DFG)	433302244	Michaela Petter
Deutsche Forschungsgemeinschaft (DFG)	423957469	Michaela Petter
Universities Australia-Deutscher Akademischer Austauschdienst		Michael F. Duffy

## AUTHOR CONTRIBUTIONS

Suffian Azizan, Data curation, Formal analysis, Investigation, Methodology, Validation, Writing – original draft, Writing – review and editing | Shamista A. Selvarajah, Conceptualization, Data curation, Formal analysis, Investigation, Methodology, Validation, Visualization, Writing – review and editing | Jingyi Tang, Formal analysis, Investigation, Methodology, Writing – review and editing | Myriam D. Jeninga, Formal analysis, Investigation, Methodology, Visualization, Writing – review and editing | Danae Schulz, Data curation, Formal analysis, Software, Visualization, Writing – review and editing | Kapil Pareek, Investigation, Methodology | Tamara Herr, Investigation | Karen P. Day, Resources, Writing – review and editing | Tania F. De Koning-Ward, Funding acquisition, Supervision, Writing – review and editing | Michaela Petter, Conceptualization, Formal analysis, Investigation, Methodology, Resources, Supervision, Writing – review and editing | Michael F. Duffy, Conceptualization, Data curation, Formal analysis, Funding acquisition, Investigation, Methodology, Project administration, Resources, Supervision, Visualization, Writing – original draft, Writing – review and editing

## DATA AVAILABILITY

All sequences are available as BioProject [PRJNA1023675](https://www.ncbi.nlm.nih.gov/bioproject/PRJNA1023675).

## ADDITIONAL FILES

The following material is available [online](#).

### Supplemental Material

**Fig. S1 (mBio02014-23-s0001.pdf).** Anti-Pf H2A.Zac and anti-Pf H2B.Zac do not bind acetylated H3 and H4 peptides.

**Fig. S2 (mBio02014-23-s0002.pdf).** Spearman correlation heatmaps.

**Fig. S3 (mBio02014-23-s0003.pdf).** Total and acetylated Pf H2A.Z and Pf H2B.Z enrichment in heterochromatin.

**Fig. S4 (mBio02014-23-s0004.pdf).** Total and acetylated Pf H2A.Z and Pf H2B.Z are antagonized by PfSir2B at heterochromatin boundaries.

**Fig. S5 (mBio02014-23-s0005.pdf).** Pf H2A.Z and Pf H2B.Z are enriched at transcribed *var* gene promoters and *var* introns.

**Fig. S6 (mBio02014-23-s0006.pdf).** Pf H2A.Z is deacetylated by class I and II HDACs.

## REFERENCES

- WHO. 2022. World Malaria Report.
- Bozdech Z, Llinás M, Pulliam BL, Wong ED, Zhu J, DeRisi JL. 2003. The transcriptome of the intraerythrocytic developmental cycle of *Plasmodium falciparum*. *PLoS Biol*. 1:E5. <https://doi.org/10.1371/journal.pbio.0000005>
- Painter HJ, Chung NC, Sebastian A, Albert I, Storey JD, Llinás M. 2018. Genome-wide real-time *in vivo* transcriptional dynamics during *Plasmodium falciparum* blood-stage development. *Nat Commun* 9:2656. <https://doi.org/10.1038/s41467-018-04966-3>
- Balaji S, Babu MM, Iyer LM, Aravind L. 2005. Discovery of the principal specific transcription factors of apicomplexa and their implication for the evolution of the AP2-Integrase DNA binding domains. *Nucleic Acids Res* 33:3994–4006. <https://doi.org/10.1093/nar/gki709>
- Bischoff E, Vaquero C. 2010. *In silico* and biological survey of transcription-associated proteins implicated in the transcriptional machinery during the erythrocytic development of *Plasmodium falciparum*. *BMC Genomics* 11:34. <https://doi.org/10.1186/1471-2164-11-34>
- Salcedo-Amaya AM, van Driel MA, Alako BT, Trelle MB, van den Elzen AMG, Cohen AM, Janssen-Megens EM, van de Vegte-Bolmer M, Selzer RR, Iniguez AL, Green RD, Sauerwein RW, Jensen ON, Stunnenberg HG. 2009. Dynamic histone H3 epigenome marking during the intraerythrocytic cycle of *Plasmodium falciparum*. *Proc Natl Acad Sci U S A* 106:9655–9660. <https://doi.org/10.1073/pnas.0902515106>
- Bártfai R, Hoeijmakers WAM, Salcedo-Amaya AM, Smits AH, Janssen-Megens E, Kaan A, Treeck M, Gilberger T-W, Françojs K-J, Stunnenberg HG. 2010. H2A.Z demarcates intergenic regions of the *Plasmodium falciparum* epigenome that are dynamically marked by H3K9ac and H3K4me3. *PLoS Pathog* 6:e1001223. <https://doi.org/10.1371/journal.ppat.1001223>
- Petter M, Lee CC, Byrne TJ, Boysen KE, Volz J, Ralph SA, Cowman AF, Brown GV, Duffy MF. 2011. Expression of *P. falciparum* *var* genes involves exchange of the histone variant H2A.Z at the promoter. *PLoS Pathog* 7:e1001292. <https://doi.org/10.1371/journal.ppat.1001292>
- Hoeijmakers WAM, Salcedo-Amaya AM, Smits AH, Françojs K-J, Treeck M, Gilberger T-W, Stunnenberg HG, Bártfai R. 2013. H2A.Z/H2B.Z double-variant Nucleosomes inhabit the AT-rich promoter regions of the *Plasmodium falciparum* genome. *Mol Microbiol* 87:1061–1073. <https://doi.org/10.1111/mmi.12151>
- Petter M, Selvarajah SA, Lee CC, Chin WH, Gupta AP, Bozdech Z, Brown GV, Duffy MF. 2013. H2A.Z and H2B.Z double-variant nucleosomes define Intergenic regions and dynamically occupy *var* gene promoters in the malaria parasite *Plasmodium falciparum*. *Mol Microbiol* 87:1167–1182. <https://doi.org/10.1111/mmi.12154>
- Tang J, Chisholm SA, Yeoh LM, Gilson PR, Papenfuss AT, Day KP, Petter M, Duffy MF. 2020. Histone modifications associated with gene expression and genome accessibility are dynamically enriched at *Plasmodium*

*falciparum* regulatory sequences. *Epigenetics Chromatin* 13:50. <https://doi.org/10.1186/s13072-020-00365-5>

12. Li B, Pattenden SG, Lee D, Gutiérrez J, Chen J, Seidel C, Gerton J, Workman JL. 2005. Preferential occupancy of Histone variant H2AZ at inactive promoters influences local histone modifications and chromatin remodeling. *Proc Natl Acad Sci U S A* 102:18385–18390. <https://doi.org/10.1073/pnas.0507975102>
13. Park YJ, Dyer PN, Tremethick DJ, Luger K. 2004. A new fluorescence resonance energy transfer approach demonstrates that the Histone variant H2AZ stabilizes the histone octamer within the nucleosome. *J Biol Chem* 279:24274–24282. <https://doi.org/10.1074/jbc.M313152200>
14. Chen P, Zhao J, Wang Y, Wang M, Long H, Liang D, Huang L, Wen Z, Li W, Li X, Feng H, Zhao H, Zhu P, Li M, Wang Q, Li G. 2013. H3.3 actively marks enhancers and primes gene transcription via opening higher-ordered Chromatin. *Genes Dev* 27:2109–2124. <https://doi.org/10.1101/gad.222174.113>
15. Lewis TS, Sokolova V, Jung H, Ng H, Tan D. 2021. Structural basis of chromatin regulation by histone variant H2A.Z. *Nucleic Acids Res* 49:11379–11391. <https://doi.org/10.1093/nar/gkab907>
16. Cole L, Kurscheid S, Nekrasov M, Domaschenz R, Vera DL, Dennis JH, Tremethick DJ. 2021. Multiple roles of H2A.Z in regulating promoter Chromatin architecture in human cells. *Nat Commun* 12:2524. <https://doi.org/10.1038/s41467-021-22688-x>
17. Thambirajah AA, Dryhurst D, Ishibashi T, Li A, Maffey AH, Ausiò J. 2006. H2A.Z stabilizes chromatin in a way that is dependent on core histone acetylation. *J Biol Chem* 281:20036–20044. <https://doi.org/10.1074/jbc.M601975200>
18. Ishibashi T, Dryhurst D, Rose KL, Shabanowitz J, Hunt DF, Ausiò J. 2009. Acetylation of vertebrate H2A.Z and its effect on the structure of the nucleosome. *Biochemistry* 48:5007–5017. <https://doi.org/10.1021/bi900196c>
19. Valdés-Mora F, Song JZ, Statham AL, Strbenac D, Robinson MD, Nair SS, Patterson KL, Tremethick DJ, Stirzaker C, Clark SJ. 2012. Acetylation of H2A.Z is a key epigenetic modification associated with gene deregulation and epigenetic remodeling in cancer. *Genome Res* 22:307–321. <https://doi.org/10.1101/gr.118919.110>
20. Ku M, Jaffe JD, Koche RP, Rheinbay E, Endoh M, Koseki H, Carr SA, Bernstein BE. 2012. H2A.Z landscapes and dual modifications in pluripotent and multipotent stem cells underlie complex genome regulatory functions. *Genome Biol* 13:R85. <https://doi.org/10.1186/gb-2012-13-10-85>
21. Dalvai M, Bellucci L, Fleury L, Lavigne AC, Moutahir F, Bystricky K. 2013. H2A.Z-dependent crosstalk between enhancer and promoter regulates cyclin D1 expression. *Oncogene* 32:4243–4251. <https://doi.org/10.1038/onc.2012.442>
22. Halley JE, Kaplan T, Wang AY, Kobor MS, Rine J. 2010. Roles for H2A.Z and its acetylation in GAL1 transcription and gene induction, but not GAL1-transcriptional memory. *PLoS Biol* 8:e1000401. <https://doi.org/10.1371/journal.pbio.1000401>
23. Bruce K, Myers FA, Mantouvalou E, Lefevre P, Greaves I, Bonifer C, Tremethick DJ, Thorne AW, Crane-Robinson C. 2005. The replacement histone H2A.Z in a hyperacetylated form is a feature of active genes in the chicken. *Nucleic Acids Res* 33:5633–5639. <https://doi.org/10.1093/nar/gki874>
24. Millar CB, Grunstein M. 2006. Genome-wide patterns of histone modifications in yeast. *Nat Rev Mol Cell Biol* 7:657–666. <https://doi.org/10.1038/nrm1986>
25. Tramantano M, Sun L, Au C, Labuz D, Liu Z, Chou M, Shen C, Luk E. 2016. Constitutive turnover of histone H2A.Z at yeast promoters requires the preinitiation complex. *Elife* 5:e14243. <https://doi.org/10.7554/elife.14243>
26. Brahma S, Udagama MI, Kim J, Hada A, Bhardwaj SK, Hailu SG, Lee TH, Bartholomew B. 2017. InQ80 exchanges H2A.Z for H2A by translocating on DNA proximal to histone dimers. *Nat Commun* 8:15616. <https://doi.org/10.1038/ncomms15616>
27. Miao J, Fan Q, Cui L, Li J, Li J, Cui L. 2006. The malaria parasite *Plasmodium falciparum* histones: organization, expression, and acetylation. *Gene* 369:53–65. <https://doi.org/10.1016/j.gene.2005.10.022>
28. Trelle MB, Salcedo-Amaya AM, Cohen AM, Stunnenberg HG, Jensen ON. 2009. Global histone analysis by mass spectrometry reveals a high content of acetylated lysine residues in the malaria parasite *Plasmodium falciparum*. *J Proteome Res* 8:3439–3450. <https://doi.org/10.1021/pr9000898>
29. Cobbold SA, Santos JM, Ochoa A, Perlman DH, Llinás M. 2016. Proteome-wide analysis reveals widespread lysine acetylation of major protein complexes in the malaria parasite. *Sci Rep* 6:19722. <https://doi.org/10.1038/srep19722>
30. Saraf A, Cervantes S, Bunnik EM, Ponts N, Sardiú ME, Chung D-WD, Prudhomme J, Varberg JM, Wen Z, Washburn MP, Florens L, Le Roch KG. 2016. Dynamic and Combinatorial landscape of Histone modifications during the Intraerythrocytic developmental cycle of the malaria parasite. *J Proteome Res* 15:2787–2801. <https://doi.org/10.1021/acs.jproteome.6b00366>
31. Coetze N, Sidoli S, van Biljon R, Painter H, Llinás M, Garcia BA, Birkholtz L-M. 2017. Quantitative chromatin proteomics reveals a dynamic histone post-translational modification landscape that defines asexual and sexual *Plasmodium falciparum* parasites. *Sci Rep* 7:607. <https://doi.org/10.1038/s41598-017-00687-7>
32. Hoeijmakers WAM, Miao J, Schmidt S, Toenhake CG, Shrestha S, Venhuizen J, Henderson R, Birnbaum J, Ghidelli-Disse S, Drewes G, Cui L, Stunnenberg HG, Spielmann T, Bártfai R. 2019. Epigenetic reader complexes of the human malaria parasite, *Plasmodium falciparum*. *Nucleic Acids Res* 47:11574–11588. <https://doi.org/10.1093/nar/gkz1044>
33. Josling GA, Petter M, Oehring SC, Gupta AP, Dietz O, Wilson DW, Schubert T, Längst G, Gilson PR, Crabb BS, Moes S, Jenoe P, Lim SW, Brown GV, Bozdech Z, Voss TS, Duffy MF. 2015. A *Plasmodium falciparum* bromodomain protein regulates invasion gene expression. *Cell Host Microbe* 17:741–751. <https://doi.org/10.1016/j.chom.2015.05.009>
34. Santos JM, Josling G, Ross P, Joshi P, Orchard L, Campbell T, Schieler A, Cristea IM, Llinás M. 2017. Red blood cell invasion by the malaria parasite is coordinated by the PfAP2-I transcription factor. *Cell Host Microbe* 21:731–741. <https://doi.org/10.1016/j.chom.2017.05.006>
35. Quinn JE, Jeninga MD, Limm K, Pareek K, Meißgeier T, Bachmann A, Duffy MF, Petter M. 2022. The putative bromodomain protein PfBDP7 of the human malaria parasite *Plasmodium falciparum* cooperates with PfBDP1 in the silencing of variant surface antigen expression. *Front Cell Dev Biol* 10:816558. <https://doi.org/10.3389/fcell.2022.816558>
36. Duraisingham MT, Voss TS, Marty AJ, Duffy MF, Good RT, Thompson JK, Freitas-Junior LH, Scherf A, Crabb BS, Cowman AF. 2005. Heterochromatin silencing and locus repositioning linked to regulation of virulence genes in *Plasmodium falciparum*. *Cell* 121:13–24. <https://doi.org/10.1016/j.cell.2005.01.036>
37. Freitas-Junior LH, Hernandez-Rivas R, Ralph SA, Montiel-Condado D, Ruvalcaba-Salazar OK, Rojas-Meza AP, Mâncio-Silva L, Leal-Silvestre RJ, Gontijo AM, Shorte S, Scherf A. 2005. Telomeric heterochromatin propagation and histone acetylation control mutually exclusive expression of antigenic variation genes in malaria parasites. *Cell* 121:25–36. <https://doi.org/10.1016/j.cell.2005.01.037>
38. Tonkin CJ, Carret CK, Duraisingham MT, Voss TS, Ralph SA, Hommel M, Duffy MF, Silva LM da, Scherf A, Ivens A, Speed TP, Beeson JG, Cowman AF. 2009. Sir2 Paralogues cooperate to regulate virulence genes and antigenic variation in *Plasmodium falciparum*. *PLoS Biol* 7:e84. <https://doi.org/10.1371/journal.pbio.1000084>
39. Coleman BL, Skillman KM, Jiang RHY, Childs LM, Altenhofen LM, Ganter M, Leung Y, Goldowitz I, Kafsack BFC, Marti M, Llinás M, Buckee CO, Duraisingham MT. 2014. A *Plasmodium falciparum* histone deacetylase regulates antigenic variation and gamete conversion. *Cell Host Microbe* 16:177–186. <https://doi.org/10.1016/j.chom.2014.06.014>
40. Deitsch KW, Calderwood MS, Wellemes TE. 2001. Cooperative silencing elements in *var* genes. *Nature* 412:875–876. <https://doi.org/10.1038/35091146>
41. Amit-Avraham I, Pozner G, Eshar S, Fastman Y, Kolevzon N, Yavin E, Dzikowski R. 2015. Antisense long noncoding RNAs regulate *var* gene activation in the malaria parasite *Plasmodium falciparum*. *Proc Natl Acad Sci U S A* 112:E982–91. <https://doi.org/10.1073/pnas.1420855112>
42. Meneghini MD, Wu M, Madhani HD. 2003. Conserved histone variant H2A.Z protects euchromatin from the ectopic spread of silent heterochromatin. *Cell* 112:725–736. [https://doi.org/10.1016/s0092-8674\(03\)00123-5](https://doi.org/10.1016/s0092-8674(03)00123-5)
43. Zhou BO, Wang SS, Xu LX, Meng FL, Xuan YJ, Duan YM, Wang JY, Hu H, Dong X, Ding J, Zhou JQ. 2010. SWR1 complex poised heterochromatin

boundaries for antisilencing activity propagation. *Mol Cell Biol* 30:2391–2400. <https://doi.org/10.1128/MCB.01106-09>

44. Bryll AR, Peterson CL. 2022. Functional interaction between the RNA exosome and the sirtuin deacetylase Hst3 maintains transcriptional homeostasis. *Genes Dev* 36:17–22. <https://doi.org/10.1101/gad.348923.121>

45. Duffy MF, Brown GV, Basuki W, Krejany EO, Noviyanti R, Cowman AF, Reeder JC. 2002. Transcription of multiple *var* genes by individual, trophozoite-stage *Plasmodium falciparum* cells expressing a chondroitin sulphate A binding phenotype. *Mol Microbiol* 43:1285–1293. <https://doi.org/10.1046/j.1365-2958.2002.02822.x>

46. Jeninga MD, Tang J, Selvarajah SA, Maier AG, Duffy MF, Petter M. 2023. *Plasmodium falciparum* gametocytes display global chromatin remodelling during sexual differentiation. *BMC Biol.* 21:65. <https://doi.org/10.1186/s12915-023-01568-4>

47. Anonymous.!!! INVALID CITATION !!! 7, 11).

48. Nardelli SC, Silmon de Monerri NC, Vanagas L, Wang X, Tampaki Z, Sullivan WJ Jr, Angel SO, Kim K. 2022. Genome-wide localization of histone variants in *Toxoplasma gondii* implicates variant exchange in stage-specific gene expression. *BMC Genomics* 23:128. <https://doi.org/10.1186/s12864-022-08338-6>

49. Zhang Y, Liu T, Meyer CA, Eeckhoute J, Johnson DS, Bernstein BE, Nusbaum C, Myers RM, Brown M, Li W, Liu XS. 2008. Model-based analysis of ChIP-Seq (MACS). *Genome Biol* 9. <https://doi.org/10.1186/gb-2008-9-9-r137>

50. Lun ATL, Smyth GK. 2016. csaaw: a bioconductor package for differential binding analysis of ChIP-seq data using sliding windows. *Nucleic Acids Res* 44:e45. <https://doi.org/10.1093/nar/gkv1191>

51. Avraham I, Schreier J, Dzikowski R. 2012. Insulator-like pairing elements regulate silencing and mutually exclusive expression in the malaria parasite *Plasmodium falciparum*. *Proc Natl Acad Sci U S A* 109:E3678–86. <https://doi.org/10.1073/pnas.1214572109>

52. Darkin-Rattray SJ, Gurnett AM, Myers RW, Dulski PM, Crumley TM, Alocco JJ, Cannova C, Meinke PT, Colletti SL, Bednarek MA, Singh SB, Goetz MA, Dombrowski AW, Polishook JD, Schmatz DM. 1996. Apicidin: a novel antiprotozoal agent that inhibits parasite histone deacetylase. *Proc Natl Acad Sci U S A* 93:13143–13147. <https://doi.org/10.1073/pnas.93.23.13143>

53. Andrews KT, Tran TN, Wheatley NC, Fairlie DP. 2009. Targeting histone deacetylase inhibitors for anti-malarial therapy. *Curr Top Med Chem* 9:292–308. <https://doi.org/10.2174/156802609788085313>

54. Gaimo BD, Ferrante F, Herchenröther A, Hake SB, Borggrefe T. 2019. The histone variant H2A.Z in gene regulation. *Epigenetics Chromatin* 12:37. <https://doi.org/10.1186/s13072-019-0274-9>

55. Kensche PR, Hoeijmakers WAM, Toenhake CG, Bras M, Chappell L, Berriman M, Bárta R. 2016. The nucleosome landscape of *Plasmodium falciparum* reveals chromatin architecture and dynamics of regulatory sequences. *Nucleic Acids Res* 44:2110–2124. <https://doi.org/10.1093/nar/gkv1214>

56. Weber CM, Ramachandran S, Henikoff S. 2014. Nucleosomes are context-specific, H2A.Z-modulated barriers to RNA polymerase. *Mol Cell* 53:819–830. <https://doi.org/10.1016/j.molcel.2014.02.014>

57. Horikoshi N, Arimura Y, Taguchi H, Kurumizaka H. 2016. Crystal structures of heterotypic nucleosomes containing histones H2A.Z and H2A. *Open Biol* 6:160127. <https://doi.org/10.1098/rsob.160127>

58. Weber CM, Henikoff JG, Henikoff S. 2010. H2A.Z nucleosomes enriched over active genes are homotypic. *Nat Struct Mol Biol* 17:1500–1507. <https://doi.org/10.1038/nsmb.1926>

59. Jin C, Felsenfeld G. 2007. Nucleosome stability mediated by histone variants H3.3 and H2A.Z. *Genes Dev* 21:1519–1529. <https://doi.org/10.1101/gad.154770>

60. Jin C, Zang C, Wei G, Cui K, Peng W, Zhao K, Felsenfeld G. 2009. “H3.3/H2A.Z double variant-containing nucleosomes mark ‘nucleosome-free regions’ of active promoters and other regulatory regions”. *Nat Genet* 41:941–945. <https://doi.org/10.1038/ng.409>

61. Fraschka SA-K, Henderson RWM, Bárta R. 2016. H3.3 demarcates GC-rich coding and subtelomeric regions and serves as potential memory mark for virulence gene expression in *Plasmodium falciparum*. *Sci Rep* 6:31965. <https://doi.org/10.1038/srep31965>

62. Duffy MF, Selvarajah SA, Josling GA, Petter M. 2014. Epigenetic regulation of the *Plasmodium falciparum* genome. *Brief Funct Genomics* 13:203–216. <https://doi.org/10.1093/bfgp/elt047>

63. Merrick CJ, Durasinh MT. 2007. *Plasmodium falciparum* Sir2: an unusual sirtuin with dual histone deacetylase and ADP-ribosyltransferase activity. *Eukaryot Cell* 6:2081–2091. <https://doi.org/10.1128/EC.00114-07>

64. Babiarz JE, Halley JE, Rine J. 2006. Telomeric Heterochromatin boundaries require NuA4-dependent acetylation of histone variant H2A.Z in *Saccharomyces cerevisiae*. *Genes Dev* 20:700–710. <https://doi.org/10.1101/gad.1386306>

65. Calderwood MS, Gannoun-Zaki L, Wellemes TE, Deitsch KW. 2003. *Plasmodium falciparum* var genes are regulated by two regions with separate promoters, one upstream of the coding region and a second within the intron. *J Biol Chem* 278:34125–34132. <https://doi.org/10.1074/jbc.M213065200>

66. Duffy MF, Byrne TJ, Elliott SR, Wilson DW, Rogerson SJ, Beeson JG, Noviyanti R, Brown GV. 2005. Broad analysis reveals a consistent pattern of *var* gene transcription in *Plasmodium falciparum* repeatedly selected for a defined adhesion phenotype. *Mol Microbiol* 56:774–788. <https://doi.org/10.1111/j.1365-2958.2005.04577.x>

67. Duffy MF, Tang J, Sumardi F, Nguyen HHT, Selvarajah SA, Josling GA, Day KP, Petter M, Brown GV. 2017. Activation and clustering of a *Plasmodium falciparum* *var* gene are affected by subtelomeric sequences. *FEBS J* 284:237–257. <https://doi.org/10.1111/febs.13967>

68. Tonkin-Hill GQ, Trianty L, Noviyanti R, Nguyen HHT, Sebayang BF, Lampah DA, Marfurt J, Cobbold SA, Rambhatla JS, McConville MJ, Rogerson SJ, Brown GV, Day KP, Price RN, Anstey NM, Papenfuss AT, Duffy MF. 2018. The *Plasmodium falciparum* transcriptome in severe malaria reveals altered expression of genes involved in important processes including surface antigen-encoding *var* genes. *PLoS Biol* 16:e2004328. <https://doi.org/10.1371/journal.pbio.2004328>

69. Dobin A, Davis CA, Schlesinger F, Drenkow J, Zaleski C, Jha S, Batut P, Chaisson M, Gingeras TR. 2013. STAR: ultrafast universal RNA-seq aligner. *Bioinformatics* 29:15–21. <https://doi.org/10.1093/bioinformatics/bts635>

70. Danecek P, Bonfield JK, Liddle J, Marshall J, Ohan V, Pollard MO, Whitwam A, Keane T, McCarthy SA, Davies RM, Li H. 2021. Twelve years of Samtools and BcfTools. *Gigascience* 10. <https://doi.org/10.1093/gigascience/giab008>

71. Liao Y, Smyth GK, Shi W. 2014. featureCounts: an efficient general purpose program for assigning sequence reads to genomic features. *Bioinformatics* 30:923–930. <https://doi.org/10.1093/bioinformatics/btt656>

72. Langmead B, Salzberg SL. 2012. Fast gapped-read alignment with Bowtie 2. *Nat Methods* 9:357–359. <https://doi.org/10.1038/nmeth.1923>

73. Ramírez F, Dündar F, Diehl S, Grüning BA, Manke T. 2014. deepTools: a flexible platform for exploring deep-sequencing data. *Nucleic Acids Res* 42:W187–91. <https://doi.org/10.1093/nar/gku365>

74. Robinson JT, Thorvaldsdóttir H, Winckler W, Guttman M, Lander ES, Getz G, Mesirov JP. 2011. Integrative genomics viewer. *Nat Biotechnol* 29:24–26. <https://doi.org/10.1038/nbt.1754>

75. Quinlan AR, Hall IM. 2010. BEDTools: a flexible suite of utilities for comparing genomic features. *Bioinformatics* 26:841–842. <https://doi.org/10.1093/bioinformatics/btq033>